

Author's response for manuscript bg-2018-85

Title: Ecosystem fluxes of carbonyl sulfide in an old-growth forest: temporal dynamics and responses to diffuse radiation and heat waves

This document contains the following:

1. Point by point response to reviewer 1
2. Point by point response to reviewer 2
3. Revised manuscript containing necessary changes

Thank you for considering this manuscript for potential publication in Biogeosciences.
Kindly let me know if any further information is required.

Sincerely,
Bharat Rastogi

Response to Reviewer 1

The manuscript reports a very interesting and important research concerning the relationship between carbonyl sulfide and carbon dioxide fluxes on ecosystem level and their response to diffuse radiation and heat waves. Current literature lacks the flux measurements provided by this study. This study will help fill in some knowledge gaps needed for implementing carbonyl sulfide as a constrain for the gross primary production on larger scales. Although the author had good references concerning the methods it lacks some basic information. Is the used instrument capable of correcting for the any effects due to water broadening and equally important were the surfaces chamber fluxes executed correctly? If the flow that is sucking the air out of the chambers is too high, COS depleted air from lower soil layers could distort the measurements. Concerning the concentration gradient, I was wondering why no invers lagrangian modelling was done as this method could help determine the sinks or sources within the canopy.

We thank the reviewer for providing thoughtful and detailed feedback on the manuscript. We address comments about water broadening, surface measurements and Lagrangian modelling in this response.

30-33 This statement is a bit farfetched. On what basis do you make this statement? LRU varies in your study, not only between seasons, but also as a result of changing light conditions (fraction of diffuse downwelling shortwave radiation)

Thank you for pointing this out. We have changed these lines in the abstract (lines-25-29) to say “*OCS fluxes showed a pronounced diurnal cycle, with maximum uptake during mid-day. OCS uptake was found to scale with independent measurements of CO₂ fluxes over a 60-m-tall old-growth forest in the Pacific Northwestern U.S. (45°49'13.76" N; 121°57'06.88") at daily and monthly timescales under mid-high light conditions across the growing season in 2015.*”

48 This is not entirely true, under stressed conditions plants have been reported to emit COS.
Add:

Bloem, E., et al. (2012). "Sulfur Fertilization and Fungal Infections Affect the Exchange of H₂S and COS from Agricultural Crops." *Journal of Agricultural and Food Chemistry* 60(31): 7588-7596. or other stress related OCS publication, as a heatwave might change the ratio of OCS to CO₂ uptake.

Thank you for providing the reference. We have included this (line 49).

115 If related to plant stress and photosynthesis (108), water potential would be a much better parameter to reflect the plant available water (if the parameter is available). Plant available water strongly depends on soil type and structure.

We agree with the reviewer’s comment about water potential. Unfortunately, we were not able to measure this quantity at the time of measurement.

140 My knowledge about the Los Gatos instrument is limited, but as literature tells me, the build in water correction of the instrument might not able to fully compensate for the effect of water vapor in sample air. Have you done dependency curves of gas with a known OCS concentration

at levels of different water vapor to test your instrument and the analysis routine? If not, I would strongly suggest doing this to avoid or correct for measurement errors. For further information, I recommend reading: Bunk, R., et al. (2017). "Exchange of carbonyl sulfide (OCS) between soils and atmosphere under various CO₂ concentrations." *Journal of Geophysical Research-Biogeosciences* 122(6): 1343-1358. See section 2.3, where this problem has been tackled with!

Thank you for pointing this. This was a cause of concern, we worked with the manufacturer on this, and found that while there was a slight dependence of water vapour on OCS mixing ratios, the effect was very small and likely doesn't affect measurements in this study (Fig.1).

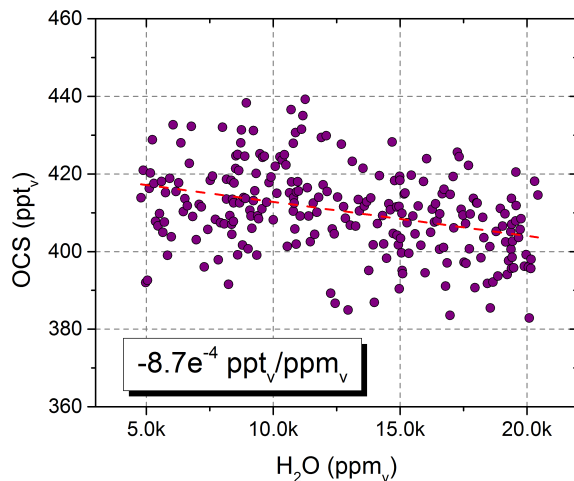


Figure 1. OCS water vapor cross-interference tested in the lab. The magnitude of this cross interference is negligible compared to observed canopy- atmosphere ecosystem exchange in this study

176 A reference suggesting only using mid-day hours would be appreciated. Didn't the cloud cover change from early morning to late evening?

Cloud cover does change during the day. However, the ratio of direct: diffuse light is also sensitive to solar zenith angles (such that the fraction of diffused light is always higher in the mornings and evenings). This is why we restrict our analyses with diffused radiation to mid-day.

181 Did you have problems applying the modified bowen ratio method? The publication cited in Commane et al. 2015 Meyers, T. P., et al. (1996). "Use of the modified Bowen- ratio technique to measure fluxes of trace gases." *Atmospheric Environment* 30(19): 3321-3329 States, that using this method might have issues when used within plant canopies. They state that "Infrequent but large energetic eddies are responsible for most of the exchange that occurs within canopies (Baldocchi and Meyers, 1991; Shaw et al., 1983). Transport by these coherent structures often leads to the counter-gradient flux structure frequently observed in crop and forest canopies." Also, why didn't you apply invers Lagrangian modelling like: Nemitz, E., et al. (2000). "Sources and sinks of ammonia within an oilseed rape canopy." *Agricultural and Forest Meteorology* 105(4): 385-404. and

Karl, T., et al. (2004). "Exchange processes of volatile organic compounds above a tropical rain

forest: Implications for modeling tropospheric chemistry above dense vegetation." *Journal of Geophysical Research: Atmospheres* (1984–2012) 109(D18).

You could even get the information about the source or sink strength of layers within your canopy.

Thank you for your suggestions and accompanying references. We have been trying to use an inverse Lagrangian/ Eulerian model to address this very problem. This is an ongoing project, we have had severe challenges in parametrizing a model that is able to estimate the wind profile and other parameters (such as eddy diffusivity) through the tall old-growth canopy. We hope to address this, and report these in a future study.

232 Even though you reference Falk et al. (2008) state that you are using a night time flux partitioning method that has been optimized to the field site. The LRU in this study will be used by modelers and I think the information from what the LRU is calculated is crucial.

We agree and have included this information (lines 228-229).

246 Are you using the Licor 8100 as flow through chamber with ambient air able to enter the chamber while you suck out the air at another end? If so, is the flowrate of 3 liters per minute not too much? How big were the openings of the chamber where ambient air was allowed to enter the chamber? If the flowrate is too high, air would be sucked out of the soil which would alter the fluxes you measure. Have you done differential pressure measurements like: Kitz, F., et al. (2017). "In situ soil COS exchange of a temperate mountain grassland under simulated drought." *Oecologia*: 1-10.

Yes, we agree with the reviewer on the issue of high flow rate. However, in contrast to other chambers, there is a vent on the top of the Li-Cor 8100 soil chamber that allows equalization of pressure between the inside and outside of the chamber. This consists of an always-open tube with a specially designed flow path to keep pressures stable even in windy conditions (Xu et al., 2006).

Xu, L., Furtaw, M. D., Madsen, R. A., Garcia, R. L., Anderson, D. J., & McDermitt, D. K. (2006). On maintaining pressure equilibrium between a soil CO₂ flux chamber and the ambient air. *Journal of Geophysical Research Atmospheres*, 111(8), 1–14. <https://doi.org/10.1029/2005JD006435>

251 Was it statistically indistinguishable, then write so.

Yes, thank you. We have included this (line 241).

286 Fig 2b-c instead of 2b

Changed accordingly.

307 Inverse lagrangian modelling could answer this question. Again, why not apply it?

Kindly see comment above.

311 Fig 2c add FCO₂ to ylabel

Changed accordingly.

346 There is no soil moisture in plot 4 which would help the reader see this correlation. Is there statistical evidence or just a trend?

We have included a figure (Fig. 3) that shows this relationship.

363 To make this statement you would have to compare the soil fluxes of your site with the publications. In your case, you have a combination of soil plus understory plants and mosses which could compensate for a soil emission. (As you stated in line 271: “The influence of the developed soil on site 1 is therefore considered minimal.”). I would use the citation you used to tell that no soil emissions are expected at your site.

We have included the relevant citation (lines 354-355).

373 In line 363 you write that you haven’t observed any OCS emission, I guess you meant uptake in line 373?

We mean to say that OCS uptake was correlated with CO₂ emissions.

388 Please state what the error bars stand for (I assume standard deviation).

Noted accordingly (line 371).

394 5b-c (a would be VPD)

Changed accordingly.

424 As NEE includes both, GPP and RECO, are you saying both components are increasing during the peak growing season, or did you want to refer to the CO₂ uptake only?

We have changed this to “increase in CO₂ uptake” (line 406).

123 mid-day VPDa (c) and soil moisture instead of Mid-day VPDa (c) and Soil moisture

Changed accordingly.

225 When this condition was not met (e.g. at nighttime), fluxes were calculated by integrating the rate of change in hourly OCS mixing ratios through the entire profile. — skip using

We have removed storage flux estimates from estimation of canopy-scale leaf OCS flux.

152 from instead of form

Changed accordingly.

Response to reviewer 2

“Rastogi et al. present observed patterns of OCS uptake in an old-growth forest during 2015. Their observations are consistent with previous studies in similar ecosystems, and are valuable in corroborating those studies and in confirming that the community’s general understanding of OCS uptake holds in old-growth forests. The methods seem valid, subject to some concerns noted below. The manuscript is easy to read and clearly organized. This is not a manuscript that presents new insights or methods.”

We thank the reviewer for a very thoughtful and detailed response to our submitted manuscript. However, we would like to disagree that this method presents no new insights or methods. In this work, we propose a simple model to estimate ecosystem- scale leaf OCS fluxes from concentration measurements, using other novel measurements, such as direct measurements of canopy skin temperature, using a thermal camera. This model is based on a theoretical framework laid out by Seibt et al., (2010) and Wohlfahrt et al., 2012), and supported by other seminal ecosystem-scale studies relating OCS uptake to plant productivity or GPP (Commane et al., 2015) and stomatal conductance (Wehr et al., 2017). In addition, we show the response of inferred OCS fluxes to the diffuse fraction of downwelling radiation, as well as the response of OCS fluxes to sequential heatwaves. These responses have not been reported for any ecosystems as yet, and we hope they provide important constraints on the use of OCS as a tracer for stomatal conductance and ultimately GPP.

“Unfortunately, the inferences drawn from the observations in the manuscript are not quantitatively supported. In particular, the inferences about stomatal responses to soil moisture and heat waves seem to be not only unsupported but also incorrect (see below). The core weakness of the manuscript, which contributes to the inference problem just mentioned, is that it is overly descriptive in terms of both the analysis and the writing. In terms of the analysis, 5 of the 6 figures (and all but subsection 3.4 of the text) present time series of data, and the associated analysis is restricted entirely to ‘eyeballing’ correlations between those time series. The authors do not calculate correlation coefficients, or use multiple regression or a simple model to support their causal inferences. In terms of the writing, many patterns in the data are described in the text even though they aren’t clearly connected to any conclusions. The manuscript would be more effective if it were to focus on what was learned from the data, referring to the data as necessary to support those findings. Other patterns could be gleaned from figures or tables by any reader with a particular interest.”

We appreciate these suggestions and have reworked specific parts of the manuscript to provide more quantitative comparisons, as well as changed the language of our study that relates to soil moisture. We have also tidied up the manuscript so that it reads more cleanly.

Specific Comments:

“- lines 193-195: This justification doesn't make sense to me. The resistance to turbulent eddy transport through open air from 70m to 60m should be much less than the resistance to eddy transport through the dense canopy from 60m to the leaf surfaces. If the aim is to establish the gradient across only the stomata, then using 60m instead of 70m hardly helps. The full transport resistance from the tower top to the substomatal cavity of some particular leaf is $r_{ac} + r_{wc} + r_{lbl} + r_s$, where r_{ac} and r_{wc} are the above-canopy and within-canopy turbulent eddy resistances, r_{lbl} is the leaf boundary layer resistance, and r_s is the stomatal resistance. Of these, r_{ac} is probably negligible, r_s is probably most limiting, and r_{lbl} is probably second most limiting. The authors appear to have neglected r_{lbl} and r_{wc} , so that their G_c is not exactly the canopy-scale stomatal conductance but rather a canopy-scale combination of the stomatal, leaf boundary layer, and within-canopy turbulent eddy conductances, i.e. $G_c = 1/(r_{wc} + r_{lbl} + r_s)$. It is possible to measure r_{ac} and some portion of r_{wc} by comparing concentration measurements within the canopy to those above the canopy and using flux = conductance x gradient; this approach ought to be superior to using the theoretical u^2/u . In any case, the authors should clarify what they mean by “the” boundary layer, as the boundary layer that is usually discussed in the context of stomatal uptake is the leaf boundary layer, i.e. the thin layer of stagnant air against the surface of individual leaves, through which gas transport is substantially diffusive rather than advective or convective. Transport through the canopy airspace, or the 10m above the canopy, on the other hand, will not be diffusive at all. “

We would again like to thank the reviewer for such a carefully detailed and clear comment regarding conductance. We have rephrased this text in the original manuscript, which we acknowledge was incorrect. We agree with the reviewer that the transport between 70-60m is in fact turbulent (and therefore more related to r_{ac} than to r_{lbl}). The choice to use the canopy top mixing ratios is following previously published literature (Fares et al., 2012; and references therein). We are, however, not ignoring the leaf boundary layer in our formulation (i.e. eqs, 1-3). Here we argue (following previous studies, cited above) that the ratio of fluxes of two scalars (in this case, OCS and H₂O) across the leaf surface is proportional to the gradient between the ambient air and the leaf intercellular spaces, i.e.

$$\frac{F_{OCS}}{F_{H_2O}} = \frac{OCS_a - OCS_i}{(e_i - e_a) \cdot P^{-1}} \cdot 1.94^{-1} \quad (1)$$

where F_{OCS} and F_{H_2O} are fluxes of OCS and H₂O (in units of $\text{pmolm}^{-2}\text{s}^{-1}$ and $\text{mmolm}^{-2}\text{s}^{-1}$ respectively), OCS_a and OCS_i represent ambient and intercellular mixing ratios of OCS respectively (ppt), where $VPD_1 = e_i - e_a$ (e_i and e_a are intercellular and actual vapor pressure; kPa), and P is atmospheric pressure (kPa). We had incorrectly labelled saturated leaf pressure

obtained from leaf temperatures as e_s , and have now correctly labelled this as e_i (since it is the leaf intercellular spaces that are assumed to be saturated with water vapor, not the leaf surface). Finally, the factor 1.94 reflects the diffusivity ratio of OCS and H₂O.

To investigate the reviewer's concern regarding various resistances, we additionally estimated OCS fluxes according to the following equation

$$F_{OCS} = \left(\frac{1.56}{G_{bw}} + \frac{1.94}{G_{sw}} \right)^{-1} \cdot OCS_a \quad (2)$$

where G_{bw} and G_{sw} are the canopy- scale boundary layer and stomatal conductances for water vapour transport. The constants 1.56 and 1.94 are the ratios of diffusivities of OCS and H₂O under turbulent and diffusive flow (Seibt et al., 2010).

We derived G_{bw} by first estimating roughness parameters following Monin-Obukhiv similarity theory (Foken, 2006). These were then used to obtain stability parameters for momentum transport, which was finally used to estimate G_{bw} following Su et al., (2001). Code and further information can be found within the R package "bigleaf" and accompanying manual (<https://bitbucket.org/juergenknauer/bigleaf>). G_{sw} was estimated as

$$G_{sw} = (G_{cw}^{-1} - G_{bw}^{-1})^{-1} \quad (3)$$

where G_{cw} is the canopy (surface) conductance to water vapor transport. To address the reviewer's comments regarding the use of the Penman- Monteith method to estimate G_{cw} , we used a simple flux-gradient method to infer this conductance as follows:

$$G_{CW} = F_{H2O} \cdot \left(\frac{VPD}{P} \right)^{-1} \quad (4)$$

Where, VPD and P are the vapor pressure deficit and atmospheric pressure (both in units of kPa). Estimated conductances and F_{OCS} calculated using both approaches is shown in figure 1. Similar to Wehr et al., (2017), we find that the boundary layer conductance is not limiting at our site, and therefore $G_{sw} \sim G_{cw}$. Consequently, the resulting flux of OCS from the two methods of estimates of G_s are in fact not dissimilar (especially considering the variability around the means shown in Fig. 1b). Therefore, we decided to trust our simple method since it does not depend on theoretical formulations of stability.

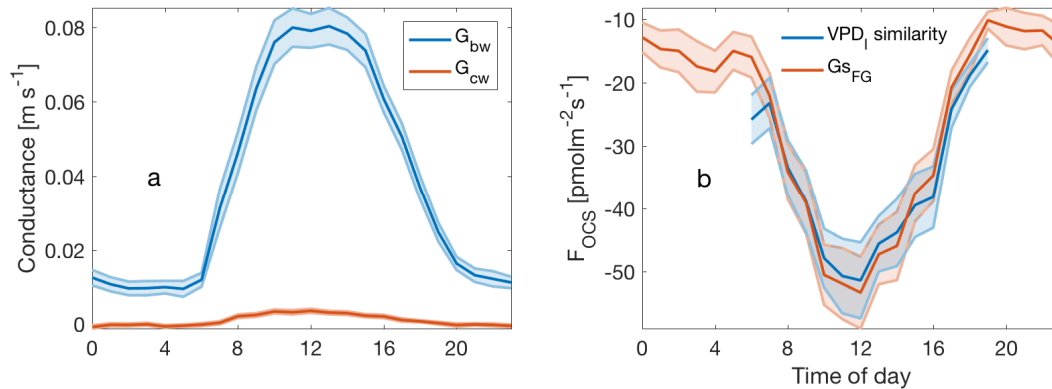


Figure 2. Mean diurnal cycles of boundary layer and canopy conductance to water vapor transport (a), and resulting OCS flux (b).

“line 223: You are talking about computing the change in canopy storage, which is a good idea, but why not do that at all times? In general, the flux through the stomata should be equal to the flux past the eddy flux sensor plus the flux into the canopy storage airspace, i.e. Eq. 1 should have a storage term appended to the right hand side (perhaps you used to have one there, as suggested by your reference to the “first term in right hand side of equation (1)” on line 221?). Here you are saying that when the eddy flux term was near zero, you considered the storage flux term. But the storage flux term might be substantial even when the eddy flux term is not near zero.”

We have revised this to exclude nighttime data, and periods when the eddy flux is near zero. In tall canopies such as our site, the portion of canopy that is coupled to the overlying atmosphere changes considerably during the day, and parts of the lower canopy are likely to be always decoupled from the upper canopy as well as above canopy air (Pyles et al., 2004). This has obvious consequences on canopy storage and venting of gases such as CO_2 and OCS. We have therefore excluded the storage flux entirely from our estimates of F_{OCS} . Moreover, change in storage flux leads to a change in mixing ratios (increase during the day), and is implicit in our formulation of F_{OCS} . We acknowledge that storage fluxes provide an important portion of the ecosystem exchange of gases such as CO_2 (and OCS) that is missed by the eddy flux measurement, but our approach doesn’t aim to infer a turbulent flux. Instead, the goal behind this study is to estimate a ‘leaf- flux’, assuming that the canopy acts like a big-leaf.

“line 236 (Eq. 6): Given the considerations about energy imbalance and the PM equation raised by Wohlfahrt et al., 2009 (Agricultural and Forest Meteorology 149, 1556– 1559) and by Wehr et al., 2017 (Biogeosciences 14, 389–401), it should be stated why this particular form of the PM equation was used (or why the PM equation was used at all instead of just using sensible heat flux measured from the tower). Those papers indicate that retrieved values of stomatal

conductance can be substantially affected by the choice of equation.”

We acknowledge the reviewer’s concern regarding the use of the Penman-Montieth method to estimate canopy conductance and have now changed the analyses to use the equation presented in eq. 4.

“- line 329: Regarding “declined precipitously with soil moisture”, it is a bit hard to tell from the color scale in Fig. 3a, but it looks like the decline in OCS (which matches the decline in G_c), is better correlated with the rise in VPD than with the drop in soil moisture. People often assume that soil moisture drives seasonal patterns in stomatal conductance (and it surely does at some sites), but it is also possible that the seasonal pattern in G_c and F_{OCS} is explained entirely by VPD (that was the finding for the mesic Harvard Forest site used in the Wehr et al., 2017 paper you cite). It would be interesting to try to disentangle those two water-related drivers here, at least with a simple regression approach.”

Yes, we agree with the reviewer on this. However, since we explicitly use VPD to estimate F_{OCS} , it would be circular for us to explain variability in F_{OCS} as a function of VPD. The idea behind showing the relationship with soils moisture was a way to link overstory canopy processes, with changes in soil moisture.

“- line 380-1: Did the estimation of ER from the tower include measurements of canopy CO_2 storage? If turbulence is low at night, most of the respired CO_2 is probably accumulating in airspaces below the eddy flux sensor.”

Flux tower estimates of CO_2 flux at the site do not incorporate storage (as computed by a profile). This is in part due to large horizontal advective losses that we are unable to estimate (Sonia Wharton, *pers. comm*) within the tall old-growth canopy. This is another reason why we chose to ignore storage estimates of OCS from this analysis.

“- line 427-9: I don’t see how this inference is connected to the preceding observations, and I don’t see any evidence in the manuscript that soil moisture (as opposed to VPD) is limiting gas exchange.”

We have changed the language in the manuscript. We also provide a simple linear regression that quantifies the relationship of F_{OCS} with soil moisture (Fig. 3b).

“- line 452-5 and 483-4: These inferences are flawed. It is not true that “canopy scale stomatal conductance during these events is dramatically reduced”. Figure 6 shows that G_c was not reduced at all during the first heat wave, and was not reduced until the end of the second heat wave, at which point the water flux also dropped. During the third heat wave, G_c was reduced,

but the water flux did not increase. Even more importantly, Gc was estimated based on the assumption that the water flux was exclusively transpiration, so it makes no sense to say that the behavior of Gc implies the increased water flux was not transpiration. If the approach used to calculate Gc is valid, then the increased water flux was indeed due to increased transpiration, on account of an increased VPDL.”

We agree with the reviewer that higher water flux is likely due to increased transpiration under high VPD, and have changed the language to reflect this (lines 425-432).

References:

- Commane, R., Meredith, L. K., Baker, I. T., Berry, J. A., Munger, J. W., Montzka, S. A., Templer, P. H., Juice, S. M., Zahniser, M. S. and Wofsy, S. C.: Seasonal fluxes of carbonyl sulfide in a midlatitude forest, *Proc. Natl. Acad. Sci.*, 112(46), 14162–14167, doi:10.1073/pnas.1504131112, 2015.
- Fares, S., Weber, R., Park, J. H., Gentner, D., Karlik, J. and Goldstein, A. H.: Ozone deposition to an orange orchard: Partitioning between stomatal and non-stomatal sinks, *Environ. Pollut.*, 169, 258–266, doi:10.1016/j.envpol.2012.01.030, 2012.
- Foken, T.: 50 years of the Monin-Obukhov similarity theory, *Boundary-Layer Meteorol.*, 119(3), 431–447, doi:10.1007/s10546-006-9048-6, 2006.
- Pyles, R. D., Paw U, K. T. and Falk, M.: Directional wind shear within an old-growth temperate rainforest: Observations and model results, *Agric. For. Meteorol.*, 125(1–2), 19–31, doi:10.1016/j.agrformet.2004.03.007, 2004.
- Seibt, U., Kesselmeier, J., Sandoval-Soto, L., Kuhn, U. and Berry, J. A.: A kinetic analysis of leaf uptake of COS and its relation to transpiration, photosynthesis and carbon isotope fractionation, *Biogeosciences*, 7(1), 333–341, doi:10.5194/bg-7-333-2010, 2010.
- Su, Z., Schmugge, T., Kustas, W. P. and Massman, W. J.: An Evaluation of Two Models for Estimation of the Roughness Height for Heat Transfer between the Land Surface and the Atmosphere, *J. Appl. Meteorol.*, 40(11), 1933–1951, doi:10.1175/1520-0450(2001)040<1933:AEOTMF>2.0.CO;2, 2001.
- Wehr, R., Commane, R., Munger, J. W., Barry Mcmanus, J., Nelson, D. D., Zahniser, M. S., Saleska, S. R. and Wofsy, S. C.: Dynamics of canopy stomatal conductance, transpiration, and evaporation in a temperate deciduous forest, validated by carbonyl sulfide uptake, *Biogeosciences*, 14(2), 389–401, doi:10.5194/bg-14-389-2017, 2017.
- Wohlfahrt, G., Brilli, F., Hörtnagl, L., Xu, X., Bingemer, H., Hansel, A. and Loreto, F.: Carbonyl sulfide (COS) as a tracer for canopy photosynthesis, transpiration and stomatal conductance: Potential and limitations, *Plant, Cell Environ.*, 35(4), 657–667, doi:10.1111/j.1365-3040.2011.02451.x, 2012.

1 **Ecosystem fluxes of carbonyl sulfide in an old-growth forest: temporal dynamics**
2 **and responses to diffuse radiation and heat waves**

3 Bharat Rastogi¹, Max Berkelhammer², Sonia Wharton³, Mary E Whelan⁴ Frederick C.
4 Meinzer⁵, David Noone⁶, and Christopher J. Still¹

5
6 ¹ Department of Forest Ecosystems and Society, Oregon State University, OR 97331,
7 USA

8 ² Department of Earth and Environmental Sciences, University of Illinois at Chicago,
9 Chicago, Illinois, USA

10 ³ Atmospheric, Earth and Energy Division, Lawrence Livermore National Laboratory,
11 7000 East Avenue, L-103, Livermore, CA 94550, USA

12 ⁴ Carnegie Institution for Science, 260 Panama St., Stanford, CA, USA, 94305

13 ⁵ USDA Forest Service, PNW Research Station, Corvallis, OR 97331, USA

14 ⁶ College of Earth, Ocean and Atmospheric Sciences, Oregon State University, OR
15 97331, USA

16 Corresponding author: Bharat Rastogi (bharat_rastogi@oregonstate.edu)

17
18 **Abstract**

19 Carbonyl sulfide (OCS) has recently emerged as a tracer for terrestrial carbon uptake.
20 While physiological studies relating OCS fluxes to leaf stomatal dynamics have been
21 established at leaf and branch scales and incorporated in global carbon cycle models, the
22 quantity of data from ecosystem-scale field studies remains limited. In this study, we
23 employ established theoretical relationships to infer ecosystem-scale **plant** OCS uptake
24 from **mixing ratio** measurements. **OCS fluxes showed a pronounced diurnal cycle, with**
25 **maximum uptake during mid-day.** OCS uptake was found to scale with independent
26 measurements of CO₂ fluxes over a 60-m-tall old-growth forest in the Pacific
27 Northwestern U.S. (45°49'13.76" N; 121°57'06.88") at **daily** and monthly timescales
28 **under mid-high light conditions** across the growing season in 2015. OCS fluxes tracked
29 changes in soil moisture, and were strongly influenced by the fraction of downwelling
30 diffuse light. **Finally, we examine the effect of sequential heatwaves on fluxes of OCS,**
31 **CO₂ and H₂O.** Our results bolster previous evidence that ecosystem OCS uptake is
32 strongly related to stomatal dynamics, and measuring this gas improves constraints on
33 estimating photosynthetic rates at the ecosystem scale.

34
35 **1. Introduction**

36 **Carbonyl Sulfide (OCS) is the most abundant sulfur gas in the atmosphere, with a mean**
37 **atmospheric concentration of ~500 ppt (parts per trillion), and therefore a significant part**
38 **of the tropospheric and stratospheric sulfur cycles, with implications for the global**
39 **radiation budget and ozone depletion (Johnson et al., 1993; Notholt et al., 2003). The**
40 **dominant sink of atmospheric OCS is vegetation (Kesselmeier and Merk, 1993; Kettle et**
41 **al., 2002; Montzka et al., 2007 and references therein), through rapid and irreversible**
42 **hydrolysis by the ubiquitous enzyme carbonic anhydrase (Protoschill-Krebs, Wilhelm, &**

Deleted: concentration

Deleted: hourly

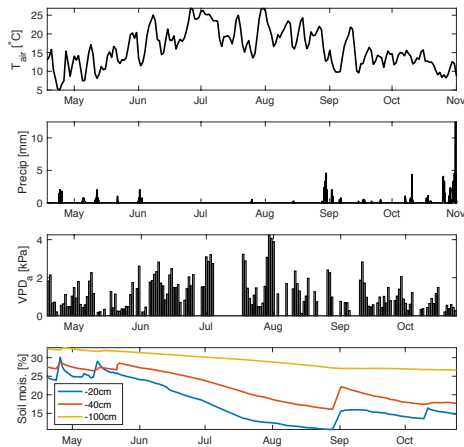
Deleted: Fluxes were also strongly affected by

Deleted: heat waves during the growing season

47 Kesselmeier, 1996; Protoschill-Krebs and Kesselmeier, 1992). Recent advances in
48 spectroscopic technology have enabled continuous in-situ measurements of OCS on
49 timescales that are relevant to understanding stomatal function at the leaf-scale (Stimler
50 et al., 2010a, 2010b), branch scale (Berkelhammer et al., 2014) and the ecosystem scale
51 (Kooijmans et al., 2017; Wehr et al., 2017). An important distinction between OCS and
52 CO₂ cycling is the absence of a retroflux from actively photosynthesizing leaves (OCS
53 emissions have been reported from stressed crops following severe fungal infection;
54 Bloem et al., 2012). However, the normalized leaf uptake ratio of OCS:CO₂ (LRU;
55 Sandoval-Soto et al., 2005) is relatively constant at medium to high light levels (Maseyk
56 et al., 2014; Stimler et al., 2010), making it an excellent proxy for quantifying plant
57 productivity (GPP; Asaf et al., 2013; Billesbach et al., 2014; Blonquist et al., 2011). On
58 the other hand, both uptake and emissions of OCS from soils have been identified
59 (Whelan et al., 2016; Sun et al., 2015; Maseyk et al., 2014; Kesselmeier et al., 1999).
60 While ecosystem-scale measurements of OCS continue to establish links between OCS
61 uptake and GPP in different ecosystems (for a comprehensive list of ecosystem scale
62 studies readers are referred to Figure 2 in Whelan et al., 2017), inconsistencies persist.
63 For example, in an oak-savanna woodland in southern France Belviso et al. (2016) found
64 that OCS exchange was strongly influenced by photosynthesis during early morning
65 hours, while meaningful values of LRU could only be calculated for a few days in the
66 early afternoons. Commane et al. (2015) were unable to explain mid-summer emissions
67 of OCS at a mid-latitude deciduous forest. Uncertainties highlighted above argue for
68 field-scale measurements of OCS in a variety of ecosystems, particularly as OCS flux
69 predictions have recently been incorporated to inform estimates of plant productivity in
70 global carbon cycle models (Campbell et al., 2017a; Hilton et al., 2017; Launois et al.,
71 2015).
72
73 OCS fluxes have not been previously reported for old-growth forests, although a recent
74 study using flask samples inferred large uptake of OCS in coastal redwood forests in
75 northern California (Campbell et al., 2017b). Rastogi et al. (in revision) found large
76 drawdowns in mixing ratios of OCS at an old growth forest in the pacific northwestern
77 U.S., and significant uptake of this gas by various components of the ecosystem (leaves,
78 soils, and epiphytes). In this study, we report estimates of OCS fluxes from an old-growth
79 forest and place them in the context of ecosystem carbon and water cycling. Additionally,
80 we investigate the response of CO₂, H₂O and OCS fluxes to changes in the fraction of
81 downwelling diffuse radiation, as well as heat wave events through the growing season.
82 Technological constraints posed limitations in measuring fast-response OCS fluxes so
83 instead we combine continuous in-situ measurements of OCS mixing ratios above and
84 within the canopy with established theoretical equations for OCS uptake (see Berry et al.,
85 2013; Commane et al., 2015; Seibt et al., 2010) to characterize OCS fluxes using a simple
86 empirical model and compare them with ecosystem uptake of CO₂ from co-located eddy
87 covariance measurements.
88
89 **2. Methods**
90 **2.1. Site Description**
91 Measurements were made at the Wind River Experimental Forest (WR), located within
92 the Gifford Pinchot National Forest in southwest Washington state, USA (45°49'13.76"

93 N; 121°57'06.88"; 371 m above sea level). The site is well studied and described in great
94 detail (Paw U et al., 2004; Shaw et al., 2004; Wharton and Falk, 2016; Winner et al.,
95 2004). The climate is classified as temperate oceanic with a strong summer drought. The
96 forest is 478 ha of preserved old-growth evergreen needle-leaf forest, with dominant tree
97 species of Douglas fir (*Pseudotsuga menziesii*) and Western hemlock (*Tsuga*
98 *heterophylla*). The tallest Douglas fir trees are between 50 and 60m, while the shade-
99 tolerant hemlocks are typically between 20-30 m high. Maximum rooting depth is 1–2 m
100 for the tallest, dominant Douglas-fir trees although most of the root biomass is
101 concentrated in the first 0.5 m (Shaw et al., 2014). The cumulative LAI is estimated to be
102 8-9 m² m⁻² (Parker et al., 2004). Additionally, the ecosystem hosts a large diversity of
103 mosses, lichens and other epiphytic plants, which play an important role in canopy OCS
104 dynamics (Rastogi et al., in revision). The soils are volcanic in origin, although most of
105 the forest surface is comprised of decaying organic matter (Shaw et al., 2004).

106
107 2.2. Study period: Measurements reported here are between April 18- Dec 31, 2015.
108 However, in early November an intake line at the top of the canopy was damaged after a
109 rainstorm. Measurements continued at the other intake heights (see sections 2.4 and 2.9).
110 Therefore, ecosystem fluxes and related analyses in this study cover 136 days between
111 April 18 and October 31, while chamber based soil fluxes are reported for the months of
112 August-December. Gaps in the time series due to analyzer maintenance correspond to Jun
113 26-28, July 6-17, August 4-7, August 24 and October 4-7. April-October roughly
114 corresponds to most of the growing season, although at this site GPP usually peaks early
115 in March-April, when soil moisture is high and ecosystem respiration flux is low, while
116 plant productivity is typically severely light and temperature limited in the months of
117 November-December (Wharton and Falk, 2016). Environmental conditions during the
118 measurement campaign are shown in Figure 1 are represent a typical Mediterranean-type
119 climate, with temperature peaking in July and minimal to no measured rainfall between
120 June and September. This results in high summertime atmospheric vapor pressure deficit
121 (VPDa), and soil moisture declines steadily through the summer period, with some
122 recharge following rare precipitation events in September and then more commonly in
123 October. The measurement period also encompasses three distinct heat waves,
124 characterized by anomalously high air temperatures and mid-day VPDa values (often
125 exceeding 4 kPa). We examine the response of OCS and CO₂ fluxes during these heat
126 waves.



Formatted: Font:(Default) Times New Roman

127
128 Figure 1. Environmental conditions at Wind River during the measurement campaign.
129 daily mean air temperature (a), precipitation (b) mid-day VPDa (c) and soil moisture
130 measured at three depths (d) are shown.

Deleted: Mid
Deleted: Soil
Deleted:).

131 2.3. CO₂ and H₂O eddy flux measurements: Carbon, water and energy fluxes have been
132 collected since 1998 at the Wind River AmeriFlux tower (US-wrc; Paw U et al. 2004).
133 For further details readers are referred to [Falk et al., \(2008; instrumentation and data](#)
134 [processing\)](#), and [Wharton et al., \(2012\)](#) and [Wharton and Falk, \(2016\)](#) for multi-year
135 carbon and water flux measurements and synthesis.

136
137 2.4. OCS measurements: A commercially available off-axis integrated cavity output
138 spectroscopy analyzer manufactured by Los Gatos Research Inc., (LGR; model 914-
139 0028) was deployed at the base of the tower in an insulated and temperature-controlled
140 shed. The instrument measures mixing ratios of OCS, CO₂, H₂O and CO simultaneously
141 at a maximal scan rate of 5Hz. The system uses a 4.87 μm cascade laser coupled to a high
142 finesse 800 cm³ optical cavity and light transmitted through the cavity is focused into a
143 cooled and amplified HgCdTe detector. OCS is detected at ~2050.40 cm⁻¹, CO₂ at
144 2050.56 cm⁻¹, CO at ~2050.86 cm⁻¹, and H₂O at ~2050.66 cm⁻¹. Pressure broadening
145 associated with changes in the concentration of water vapor in the samples is corrected
146 for in the analysis routine. Air was sampled through 0.25” diameter PFA tubing using a
147 diaphragm pump at a flow rate of 2L min⁻¹, from inlets located at 70m (at the height of
148 the eddy flux instrumentation), 60m (canopy top), 20m, 10m, and 1m. The sampling
149 frequency was 0.1Hz and the sampling interval was 5 minutes. The first minute of each
150 sampling interval was removed to avoid any inter-sampling mixing. The remaining data
151 were checked for temperature and pressure fluctuations inside the measurement chamber,
152 and a moving window filter was used to eliminate any sudden outliers in the data. Mixing
153 ratios were aggregated to provide hourly means. For detailed information regarding
154 instrumentation and the measurement readers are referred to Rastogi et al (in revision),
155 Berkelhammer et al. (2014) and Belviso et al. (2016).

159 2.5. Calibration: Calibration was performed using ambient air stored in insulated tanks as
160 a secondary reference. Air was sampled into the analyzer daily, and tank pressure was
161 routinely monitored to check for leaks. Glass flasks were randomly sampled from
162 calibration tanks and measured against a NOAA GMD reference standard. Cross-
163 referencing revealed that the accuracy of the measurement was within the reported
164 minimum uncertainty of the instrument (of 12.6 pmol mol⁻¹; [Berkelhammer et al., 2016](#)).

Deleted: form

Deleted: Berkelhammer et al., 2016)

166 2.6. Thermal Camera measurements: Leaf temperatures were measured from October 28,
167 2014 to January 28, 2016 using a FLIR A325sc thermal camera (FLIR System Inc.,
168 Wilsonville, OR), in which a FLIR IR 30-mm lens (focal length: 30.38 mm; field of
169 view: 15°×11.25°) was installed. The thermal camera has a pixel resolution of 320 × 240.
170 Within the field of view (FOV), spot sizes of a single pixel are 0.83 cm from 10-m
171 distance and 8.3 cm from 100-m distance. Manufacturer-reported errors in original
172 measured thermal temperatures are ±2 °C or ±2% of the measurements. The camera
173 model is identical to one used in another study at an AmeriFlux site in central Oregon
174 (US Me-2), and the detailed specifications can be found in [Kim et al. \(2016\)](#). To monitor
175 a larger canopy region, a pan-tilt unit (PTU) was used for motion control, allowing
176 multiple canopy thermal image acquisition within one motion cycle. We used a FLIR
177 PTU-D100E (FLIR System Inc., Wilsonville, OR; (<http://www.flir.com/mcs>)) to move the
178 thermal camera vertically and horizontally at specific pan and tilt angles. We selected
179 five pan-tilt angle (PT) positions representing the upper canopy (i.e., ~40 to 60 m above
180 the forest floor) to estimate leaf temperatures in this study.

Deleted: Kim et al. (2016

181 2.7. Diffuse light measurement and analyses: An SPN1 Sunshine Pyranometer (Delta-T
182 Devices Ltd., Cambridge, U.K.) was installed at the top of the canopy and collected direct
183 and diffuse shortwave downwelling radiation from April- December 2015. Measurements
184 were made every 1 min, and then aggregated to hourly means. We limited our analyses of
185 diffuse radiation data to include only mid-day hours (between 11am-1pm) to minimize
186 the influence of solar angles on diffuse radiation fractions. We defined three distinct
187 periods based on the ratio of diffuse radiation to total incoming solar radiation (*fdiff*).
188 Data were characterized as clear if *fdiff* < 0.2; partly cloudy if *fdiff* > 0.2 and *fdiff* < 0.8,
189 and overcast if *fdiff* > 0.8.

190 2.8. OCS flux estimation: Canopy-scale leaf OCS flux was estimated using flux-
191 gradient similarity, following Commane et al., 2015.

$$192 F_{OCS} = F_{H_2O} \cdot \frac{g_{OCS}}{g_{H_2O}} \quad (1)$$

193 where F_{OCS} , F_{H_2O} , g_{OCS} and g_{H_2O} are the fluxes and gradients of OCS and H₂O,
194 respectively. Following Seibt et al., (2010) and Berry et al., (2013), we assume that OCS
195 is irreversibly and rapidly consumed inside leaves, such that the gradient between
196 ambient air and the leaf interior effectively reduces to the ambient measured OCS mixing
197 ratio:
198

199
200 where g_{OCS} is defined as the gradient of OCS between ambient air and the leaf
201 intercellular spaces (χ is the mixing ratio of OCS and superscripts *a* and *l* refer to ambient
202

Deleted: 3

207 and leaf respectively). In our study, χ_{OCS}^a is the measured mixing ratio at the canopy top
 208 (60m) instead of above canopy (70m) to account for turbulent transport between the
 209 canopy top and air that is above the canopy top. We use vapor pressure deficit (VPD) as
 210 the corresponding gradient for H₂O, under the key assumption that the intercellular leaf
 211 surfaces are saturated with water vapor. While VPD is usually calculated using air
 212 temperature, a more accurate calculation can be performed with leaf temperatures, which
 213 can deviate significantly from air temperatures (Kim et al. 2016), leading to significant
 214 differences between the VPD of ambient air and that at the leaf surface (Fig. 2a and 3d
 215 in this study). Previously leaf temperatures have been inferred from sensible heat fluxes,
 216 wind speed and air temperatures (e.g. Wehr et al., 2017), here we use explicit
 217 measurements of leaf skin temperatures to estimate leaf-air VPD (VPD_l). Analogous to
 218 Eq (3),

$$220 \quad g_{H_2O} = \chi_{H_2O}^l - \chi_{H_2O}^a = \frac{(e_l - e_a)}{P} = \frac{VPD_l}{P}, \quad (3)$$

221 where e_l is saturation vapor pressure in the leaf sub-stomatal cavity (kPa), using leaf skin
 222 temperature, e_a is the actual vapor pressure (kPa), P is the measured atmospheric pressure
 223 (kPa) at the tower top, and $\chi_{H_2O}^l$ and $\chi_{H_2O}^a$ (ppth) are the leaf and ambient H₂O mixing
 224 ratios at the canopy top. Finally, since gradients of OCS and H₂O are estimated between
 225 ambient air and the leaf intercellular spaces, these are normalized by the ratio of
 226 diffusivities of these two species in air (Seibt et al., 2010; Wohlfahrt et al., 2012).

227 F_{H2O} was measured using eddy covariance at the tower top (70m). In high LAI forests
 228 with minimal exposed soil, such as those of the Pacific Northwest, fluxes of F_{H2O} can be
 229 treated as a good proxy for transpiration, since soil evaporation should be minimal. We
 230 excluded rainy days, as well as two days following rainfall, to only capture periods when
 231 F_{H2O} can be assumed to be dominated by transpiration. Equation (1) was evaluated only
 232 under the condition F_{H2O} > 0.2 mmol⁻²s⁻¹. We restricted our analyses to daytime, when
 233 OCS flux is assumed to be related to leaf CO₂ uptake (Maseyk et al., 2014; Wehr et al.,
 234 2017).

235 Leaf Relative uptake was calculated following Seibt et al (2010).

$$236 \quad LRU = \frac{F_{OCS}}{GPP} \cdot \frac{\chi_{CO_2}}{\chi_{OCS}}, \quad (5)$$

237 where GPP was estimated from CO₂ fluxes measured at the tower top, using a nighttime
 238 based partitioning approach (Reichstein et al., 2005), that was optimized for the site (Falk
 239 et al., 2008). Finally, canopy conductance (Gc) was estimated using a simple flux-
 240 gradient approach with the assumption that the canopy (or ecosystem) acts as a single big
 241 leaf.

$$242 \quad Gc = F_{H_2O} \cdot \frac{VPD_l}{P}, \quad (6)$$

243 2.9. Surface Fluxes: A long-term automatic soil survey chamber (Li-Cor 8100-104, 20
 244 cm diameter) was installed at three 0.03 m² surface sites in series, within 1 meter of each
 245 other. All plastic and rubber parts had been removed from the chamber and replaced with
 246 materials compatible with OCS measurements: stainless steel, PFA plastic, and Volara

Deleted: the boundary layer resistance, the effect of which is likely low in tall and heterogeneous coniferous forests.

Deleted: $\frac{(e_l - e_a)}{P}$

Deleted: 4

Deleted: where e_l is saturation vapor pressure at the leaf surface (kPa), using leaf skin temperature, e_a is the actual vapor pressure (kPa), P is the measured atmospheric pressure (Pa) at the tower top, and $\chi_{H_2O}^l$ and $\chi_{H_2O}^a$ (ppth) are the leaf and ambient H₂O mixing ratios at the canopy top. Finally, since gradients of OCS and H₂O are estimated between ambient air and the leaf intercellular spaces, these are normalized by the ratio of diffusivities of these two species in air (Seibt et al., 2010; Wohlfahrt et al., 2012). - ... [1]

Deleted: where GPP was estimated from CO₂ fluxes measured at the tower top. Finally, canopy conductance (Gc) was calculated by inverting the Penman Monteith equation (Monteith, 1965), which uses a combination of micrometeorological and eddy flux data collected above the canopy at the tower top. Gc is the canopy-scale equivalent of stomatal conductance, with the assumption that the canopy (or ecosystem) acts as a single big leaf. - ... [2]

275 foam. Blank measurements were performed in the laboratory before deployment and
276 OCS concentrations in the chamber were found to be **statistically** indistinguishable from
277 incoming ambient concentrations. The stainless-steel chamber top opened and closed
278 automatically on a timer. Gas was drawn through the chamber via a pump downstream of
279 the analyzer, and the 3 Lmin⁻¹ flow rate was confirmed with a mass flow meter. When the
280 chamber was open, ambient near-surface air was observed. When the chamber was
281 closed, trace gas concentrations reached a stable state for at least 2 minutes during the 10-
282 minute incubation time. The difference between the ambient concentration and the stable
283 closed-chamber concentration were used to calculate the surface fluxes of OCS and CO₂.

$$284 F_{forest\ floor} = M_c \Delta \chi \cdot A^{-1}, \quad (7)$$

285 where M_c is the measured flow rate into the chamber (converted from Lmin⁻¹ to mols⁻¹
286 using the ideal gas law) and $\Delta \chi$ is the difference between mixing ratios of OCS or CO₂ in
287 ambient air and the chamber and A is the surface area of the chamber. The minimum flux
288 detectable with this method was 1.2 pmolm⁻²s⁻¹ uptake or production.

289 Care was taken to select sites characteristic of the surface, which was generally springy
290 and covered in a mat of mosses and lichen. Surface flux observations were made at site 1
291 from July 6 to 16, site 2 from August 13 to October 7, and site 3 from November 6 to
292 December 2, 2015. The first site was visually similar to the subsequent two sites at the
293 surface, though the chamber base of the first site was installed into the moss layer and a
294 barely decomposed fallen tree. When a soil sample was attempted to be extracted from
295 the footprint of the chamber base, several liters of **intact** wood litter were removed. The
296 influence of the developed soil on site 1 is therefore considered minimal. Site 2 was
297 selected nearby and observations were made until a dominant tree fell on the soil
298 chamber. The chamber was repaired and re-installed a month later at site 3 and
299 observations continued without incident until the chamber was removed in advance of the
300 soil freezing.

301 3. Results and Discussion:

302 3.1. Ecosystem fluxes: The composite diurnal cycles for CO₂, water vapor and OCS and
303 fluxes are shown (Fig. 2a-c). The total ecosystem flux of OCS (F_{OCS} ; Fig 2.b.) follows a
304 pronounced diurnal cycle that peaks during daylight hours. The vertical profile of mixing
305 ratios measured throughout the canopy is also shown (right y-axis and orange lines in
306 Fig.2.b). OCS mixing ratios are highest at the canopy top and lowest near the forest floor,
307 but mixing ratios increase from the early morning to mid-afternoon. Together these
308 processes are indicative of ecosystem uptake and downward entrainment of boundary
309 layer air. While entrainment helps explain the diurnal cycle of observed mixing ratios,
310 this flux integrates to zero at daily and longer time scales (Rastogi et al., in revision). The
311 shape of the F_{OCS} curve is very similar to those of net and gross carbon fluxes (Fig 2.b-c),
312 although F_{OCS} was consistently negative throughout the 24-hour period, implying
313 ecosystem uptake during nighttime and daylight hours. While nighttime uptake of OCS
314 (mean nighttime flux $\sim -10 \pm 1$ pmolm⁻²s⁻¹) is likely due to a combination of soil,
315 epiphyte, and vascular plant uptake due from partially closed stomata, daytime uptake is
316 likely dominated by vascular plant stomatal activity. Leaf relative uptake, a ratio of
317 F_{OCS} :GPP normalized by the mean mixing ratios of OCS:CO₂, showed a strong light

Deleted:

Deleted: in tact

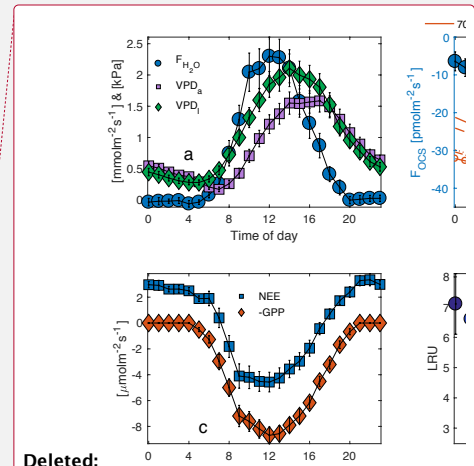
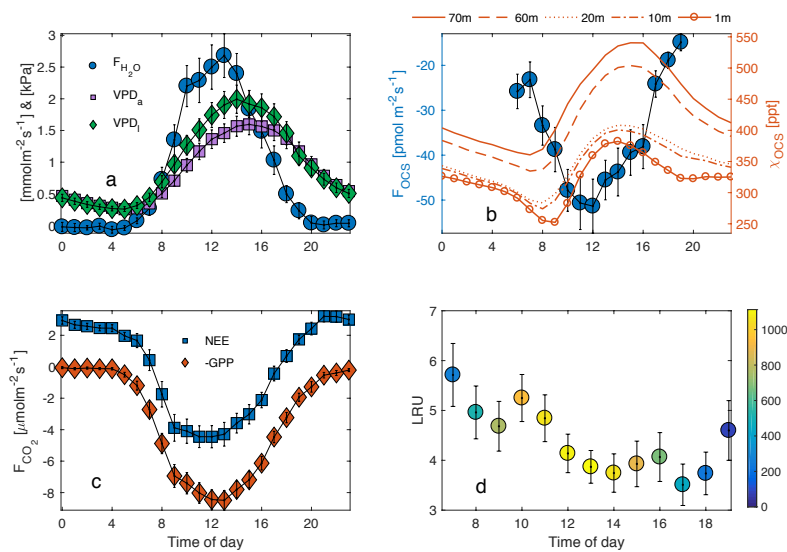
320 dependence. High-light, mid-day values ranged between 3-4, which is higher than those
 321 observed at other forest systems (Kooijmans et al., 2017; Wehr et al., 2017) but well
 322 within the spread of values obtained in a recent meta-analyses of OCS studies for
 323 vegetated ecosystems (Whelan et al., 2018). The diurnal cycle was found to be
 324 asymmetric, with peak values observed in the early morning, when stomatal conductance
 325 is likely to be high (Winner et al., 2004), but GPP is limited by low light levels. It is
 326 important to note that LRU is likely influenced by large amounts of epiphyte and
 327 understory vegetation, which assimilate OCS even at times when ecosystem CO₂ uptake
 328 is low or zero. Epiphytic assimilation of OCS is highly influenced by moisture content
 329 (Gimeno et al., 2017) and is typically higher through the night and in the early mornings
 330 at this site (Rastogi et al., in revision). Moreover, in tall old-growth forests, leaf area is
 331 vertically distributed over a much larger part of the canopy compared to other forests
 332 (Parker et al., 2004). While leaves at the canopy top exercise tight stomatal control to
 333 limit water loss and minimize hydraulic failure (Woodruff et al., 2007) leaves lower
 334 down in the canopy, including those of understory vegetation, likely impose less stomatal
 335 control of transpiration (Winner et al., 2004). Lower-canopy leaves may therefore
 336 continue to disproportionately assimilate OCS, even under low rates of carbon
 337 assimilation (as CO₂ uptake is additionally light limited).

Deleted: (Winner et al., 2004)

Deleted: (Gimeno et al., 2017)

Deleted: (Woodruff et al., 2007)

Deleted: (Winner et al., 2004)



Deleted:

Formatted: Font:(Default) Times New Roman

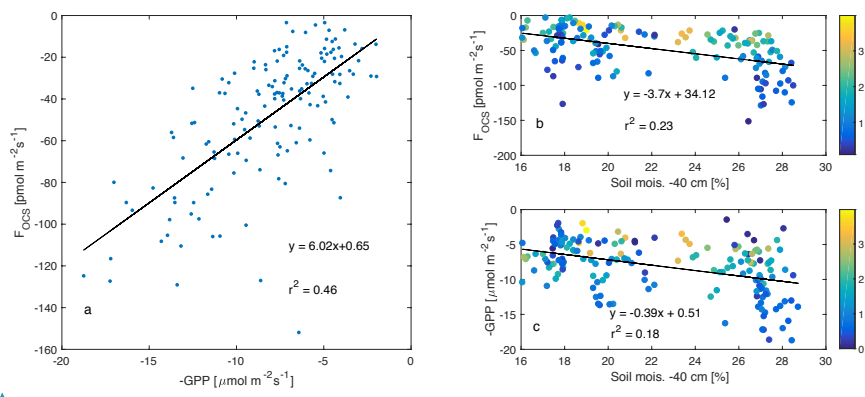
Formatted: Font:(Default) Times New Roman

338
 339 Figure 2. Diurnal cycle of H₂O flux (blue circles) and VPD estimated from air and leaf
 340 temperatures (purple squares and green diamonds respectively; a), estimated OCS flux
 341 (circles, left axis) and mixing ratio profile (right axis; b), NEE and GPP (blue squares and
 342 red diamonds; c), and leaf relative uptake (calculated only during daylight hours, colors
 343 represent Photosynthetically active radiation; d). Vertical bars indicate standard error.

344

350 3.2. Daily and seasonal dynamics: Daytime fluxes of OCS were correlated to independent
 351 estimates of GPP (Fig. 3a), and uptake of both OCS and CO₂ reduced as soil moisture
 352 declined. Variability in the relationship between fluxes of OCS and CO₂ and soil
 353 moisture was related to VPD, which fluctuated as a response of changing cloud cover
 354 (discussed later in sec. 3.4).

~~Deleted: Seasonal~~
~~Deleted: and CO₂ followed similar patterns~~
~~Deleted: -~~



~~Formatted: Font:(Default) Times New Roman~~

355 **Figure 3.** F_{OCS} was linearly correlated to GPP (plotted as a negative quantity to show
 356 ecosystem uptake; a), while both F_{OCS} and GPP reduced as a function of decreasing soil
 357 moisture (b-c). Data presented here are mid-day means, data in (b-c) are colored
 358 according to VPD.

~~Formatted: Font:12 pt, Not Bold, Font color: Text 1~~
~~Deleted:)~~
~~Deleted: ,~~
~~Deleted: .~~

360 Ecosystem uptake of OCS and CO₂ (as well as GPP) was highest in April (Fig. 4a), and
 361 declined as the soil drought progressed (Fig. 4f). Mean monthly maximum OCS flux was
 362 estimated as $-61 \pm 6 \text{ pmol m}^{-2} \text{ s}^{-1}$, while daily mean maximum GPP over this period was
 363 estimated as $10 \pm 1 \text{ } \mu\text{mol m}^{-2} \text{ s}^{-1}$ (plotted as a negative quantity in Fig. 4b to show
 364 ecosystem uptake). While the steepest declines in F_{OCS}, NEE and GPP happened between
 365 the months of May and June, F_{OCS} continued to decline through the rest of the summer,
 366 with a minimum in August, and remaining low in September and October. CO₂ fluxes
 367 flattened between June-September, before declining again in October. While uptake of
 368 OCS and CO₂ followed similar patterns, H₂O flux remained high until mid-summer (Fig.
 369 4c) before plunging in August, presumably due to a combination of high VPD (Fig. 4d)
 370 and declining soil moisture (Fig. 4f), as plants exercised greater control over stomata.
 371 This can be clearly seen in the seasonal cycle of canopy conductance (G_c; Fig. 4e). Mean
 372 monthly G_c was highest in the months of April and May, and then declined in response to
 373 increasing VPD and decreasing soil moisture, before increasing again slightly in
 374 September and October following soil recharge and decreased VPD due to precipitation
 375 events. In October, soil water recharge, several rain-free days (Fig. 1), and lower VPD
 376 (Fig. 4d) do not result in increased gas exchange, likely due to downregulation of
 377 photosynthesis (Eastman and Camm, 1995), induced by photoprotective changes in the
 378 xanthophyll cycle (Adams and Demmig-Adams, 1994).

~~Deleted: 3b~~
~~Deleted: incrementally increasing~~
~~Deleted: decreasing again in~~
~~Deleted: During mid-late summer, water vapor~~
~~Deleted: declined (Fig.3c~~
~~Deleted: responding to high VPD (peaking in July; Fig 3d).~~
~~Deleted: 3e) calculated using the Penman-Monteith method.~~
~~Deleted: precipitously with~~
~~Deleted: At the monthly scale, patterns of daytime F_{OCS} were most similar to those of G_c and followed trends in soil moisture.~~
~~Deleted: ,~~
~~Deleted: 1)~~
~~Deleted: (Eastman and Camm, 1995)~~
~~Deleted: (Adams and Demmig-Adams, 1994)~~

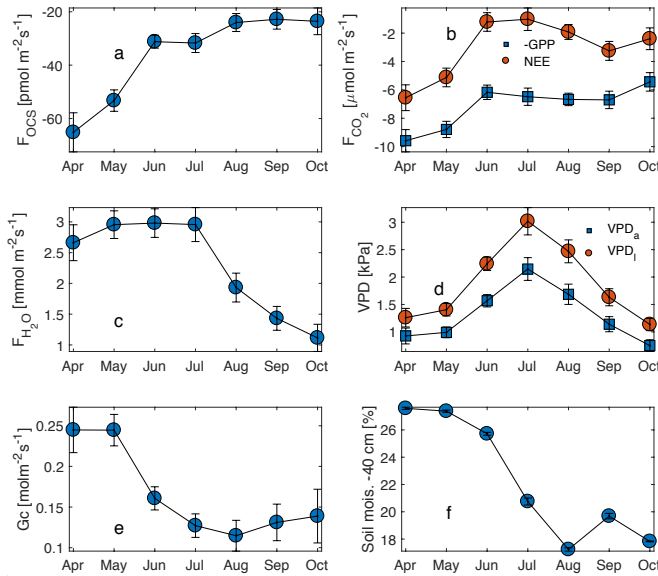
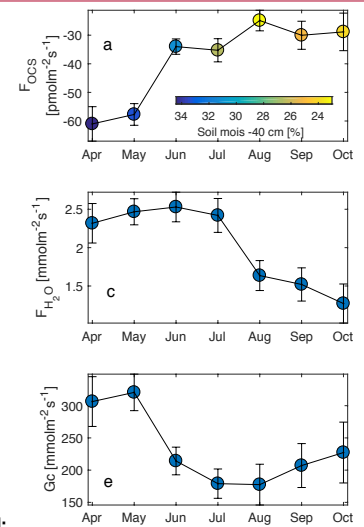


Figure 4. Monthly means for daytime F_{OCS} , NEE and -GPP (red circles and blue squares; b), water vapor flux (c), VPD_a and VPD_i (blue squares and red circles; d), canopy conductance (Gc; e), and soil moisture at -40cm depth (f). Vertical bars indicate standard error.

3.3. Surface Fluxes: Forest floor OCS fluxes were observed from 3 sites in series and within 1 m of each other. Site 1 had approximately twice the OCS uptake compared to the subsequent two sites and had a substantial layer of intact woody debris under the chamber footprint. Site 2 and 3 had OCS fluxes similar to previous surface fluxes reported for forests (Whelan et al., 2018). For all sites, there was no clear diurnal pattern. For site 2, uptake immediately following chamber installation was higher ($\sim 6 \text{ pmol m}^{-2} \text{ s}^{-1}$) than fluxes later on (all $< 6 \text{ pmol m}^{-2} \text{ s}^{-1}$) when temperatures were lower (Fig 5). Site 3 did not have high uptake after chamber installation, and had consistent fluxes between the detection limit and $-6.2 \text{ pmol m}^{-2} \text{ s}^{-1}$ for the first few weeks. When ambient air temperatures dropped below freezing, uptake remained unchanged, except for the largest uptake observed (6 to $12 \text{ pmol m}^{-2} \text{ s}^{-1}$) during two events when average air temperature fluctuated from a cooling to warming trend. Soil temperature never dropped below freezing during the experiment and was generally colder over time. We did not observe any OCS emissions from the chamber based measurements, consistent with recent studies that find that cooler, moist (Maseyk et al., 2014; Sun et al., 2016; Whelan et al., 2016) and radiation limited (Kitz et al., 2017) soils do not emit OCS.

Surface CO_2 emissions exhibited a relationship with temperature, where highest production ($\sim 25 \text{ } \mu\text{mol m}^{-2} \text{ s}^{-1}$) corresponded with temperatures $\sim 15^\circ\text{C}$, and maximum flux values decreased for warmer and colder temperatures. CO_2 emissions had a diurnal



Deleted:

Formatted: Font:(Default) Times New Roman

Formatted: Font:(Default) Times New Roman

Deleted: 3

Deleted: colored according to soil moisture at 40cm depth

Deleted: and

Deleted: .)

Deleted: 3.3. Nighttime ecosystem and Surface Fluxes: While daytime fluxes of OCS and CO_2 were indicative of seasonal changes in ecosystem productivity and conductance, F_{OCS} and F_{CO_2} were driven by different environmental conditions during the night. Ecosystem respiration is modeled based on temperature and therefore peaked in July (when air temperature was highest). Nighttime F_{OCS} however, was more related to soil moisture status (blue circles in Fig. 4a-b). Nighttime F_{OCS} was highest in April (mean = $-12.7 \pm 2.6 \text{ pmol m}^{-2} \text{ s}^{-1}$), lowest between June and August (mean = $-5.9 \pm 1.5 \text{ pmol m}^{-2} \text{ s}^{-1}$) and increased again in October (mean = $-9.7 \pm 2.2 \text{ pmol m}^{-2} \text{ s}^{-1}$). Nighttime uptake of OCS at the site is likely due to soil (see below), epiphytes (Rastogi et al., in revision; Gimeno et al., 2017), and incomplete stomatal closure (Kooijmans et al., 2017).

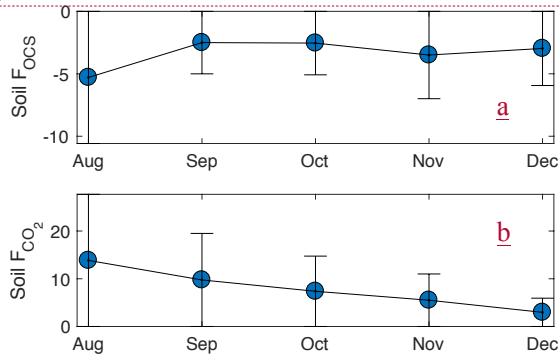
Deleted: .

Deleted: (Maseyk et al., 2014; Sun et al., 2016; Whelan et al., 2016)

Deleted: (Kitz et al., 2017)

451 pattern, with lowest emissions at night and maximum emissions in late morning to mid-
 452 afternoon. No obvious relationship emerges from CO₂ emission and OCS uptake, though
 453 the high OCS uptake events in late November and early December have a linear
 454 relationship with CO₂ emissions. For sites 2 and 3, the ratio of OCS emission to CO₂
 455 production, normalized by the concentration of OCS and CO₂ in the closed chamber, was
 456 between -0.25 and -3.5 with a mean of -1. In contrast, the same ratio for site 1 varied
 457 from -5 to -19 with a mean of -10.

458



459

460 **Figure 5.** Surface F_{OCS} and F_{CO₂} from chamber measurements (brown squares in a-b)
 461 from sites 2 and 3. Site 1 was atypical (see section 2.7) and therefore fluxes are not
 462 shown. Values for site 1 F_{OCS} and F_{CO₂} were -22 ± 0.3 pmolm⁻²s⁻¹ and -83 ± 2 μmolm⁻²s⁻¹
 463 respectively. Error bars indicate standard deviation.

464 3.4. Sensitivity to diffuse light: Mid-day fluxes of OCS and CO₂ were found to be
 465 sensitive to changes in the fraction of diffused: total incoming shortwave radiation (*f_{diff}*;
 466 Figure 6b-c). For these analyses, data were separated into three periods corresponding to
 467 early summer (DOY 109-180), mid-late summer (DOY 180-240) and early fall (DOY
 468 240-297), and binned into three categories: clear sky conditions, partly cloudy, and
 469 overcast, defined in sec. 2.7. Mid-day VPD was highest under clear sky conditions and
 470 lowest under overcast skies, but was most different across the three periods, during clear
 471 skies (Fig. 6a). Consequently, OCS and CO₂ uptake was highest (most negative fluxes)
 472 under overcast conditions during the early summer, and generally declined as *f_{diff}*
 473 decreased across all time periods (Fig. 6b-d). Across the three periods, the rate of
 474 decrease was much higher as *f_{diff}* changed from partially cloudy to clear. During the mid-
 475 late summer, however, (red diamonds in Fig. 6a-f), the diffuse light effect resulted in
 476 GPP and NEE being almost as high as during the early summer. F_{OCS} was also highest
 477 under partially cloudy skies during this time, and only showed a very weak decline under
 478 completely overcast conditions. Overall, the behavior of OCS and CO₂ fluxes was similar
 479 during the later time periods. Leaf relative uptake (LRU; calculated according to eq. 5)
 480 was lowest under partly clear skies and highest under overcast conditions. This is because
 481 under highly diffuse conditions, carbon uptake is additionally limited by light, whereas
 482 F_{OCS} is not (Wehr et al., 2017; Maseyk et al., 2014). The shape of the LRU curves can
 483 additionally be explained by examining canopy conductance (G_c; Fig. 6f), which was

483

Deleted: At the peak of the soil drought (August; Fig. 1d), nighttime ecosystem OCS flux was similar to the chamber-based surface fluxes, after which magnitudes differed by a factor of 2-3. This difference can be explained by epiphytic consumption of OCS. Epiphytes are a moisture dependent sink OCS at the site (Rastogi et al., in revision) and therefore are likely inactive during the warmest and driest part of the year. Surface fluxes of CO₂ on the other hand were much higher than ER estimated from the flux tower (blue circles in Fig. 4b). While there are issues in scaling up chamber-based estimates, these results corroborate earlier work that suggest that flux tower based estimates of ER at this site might be underestimated (Harmon et al., 2004). ... [3]

Formatted: Font:(Default) Times New Roman

Deleted: 5a-b

Deleted: 5a

Deleted: 5b

Deleted: 5a

Deleted: 5f

503 also higher under overcast skies. LRU increased with Gc across all three periods (Fig.
504 6g), and appeared to be constant for Gc greater than $\sim 400 \text{ mmolm}^{-2}\text{s}^{-1}$.

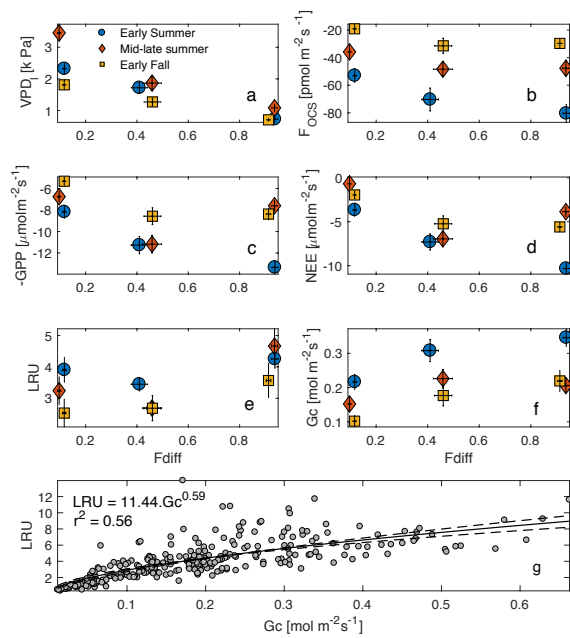
505 The diffuse light enhancement of stomatal and canopy conductance is well documented
506 across a range of forest ecosystems (Alton et al., 2007; Cheng et al., 2015; Hollinger et
507 al., 2017; Urban et al., 2007; Wharton et al., 2012). Lower VPD (Fig. 6a) and light levels
508 allow plants to keep stomata open at mid-day and continue fixing CO₂. Lower VPD
509 reduces transpirational losses, and the lack of VPD-induced partial stomatal closure
510 reduces the resistance to CO₂ diffusion into the leaf. Correspondingly, the less directional
511 nature of diffuse solar radiation allows greater penetration into the canopy, thus
512 increasing photosynthesis across the entire canopy, even as a reduction in canopy top leaf
513 photosynthesis is observed due to a reduction in total radiation. In a multi-year analysis at
514 Wind River, Wharton et al., (2012) found that cloudy and partly cloudy sky conditions
515 during the peak-growing season lead to an increase in CO₂ uptake. During our study, Gc
516 was generally higher in the early growing season, but increased as sky conditions
517 changed from clear skies to overcast. This increase was similar across the three time
518 periods, even as the response of OCS and CO₂ fluxes was different across these periods.
519 This indicates that declining soil moisture (Fig. 3b-c) likely limits gas exchange as the
520 summer progresses, even as canopy conductance can be reasonably high under overcast
521 skies.

Deleted: 5g

Deleted: The diffuse light enhancement of stomatal and canopy conductance is well documented across a range of forest ecosystems (Alton et al., 2007; Cheng et al., 2015; Hollinger et al., 2017; Urban et al., 2007; Wharton et al., 2012). Lower VPD (Fig. 5a) and light levels allow plants to keep stomata open at mid-day and continue fixing CO₂. Lower VPD reduces transpirational losses, and the lack of VPD-induced partial stomatal closure reduces the resistance to CO₂ diffusion into the leaf. Correspondingly, the less directional nature of diffuse solar radiation allows greater penetration into the canopy, thus increasing photosynthesis across the entire canopy, even as a reduction in canopy top leaf photosynthesis is observed due to a reduction in total radiation. In a multi-year analysis at Wind River, Wharton et al., (2012) found that cloudy and partly cloudy sky conditions during the peak-growing season lead to an enhancement of NEE. During our study, Gc was generally higher in the early growing season, but increased as sky conditions changed from clear skies to overcast. This increase was similar across the three time periods, even as the response of OCS and CO₂ fluxes was different across these periods. This indicates that declining soil moisture (Fig. 1d) likely limits gas exchange as the summer progresses, even as canopy conductance can be reasonably high under overcast skies. -

... [4]

Formatted: Font:(Default) Times New Roman



Formatted: Font:(Default) Times New Roman

Deleted: 5
Deleted: VPDa

Deleted: 400 mmolm
Deleted:

Deleted: (Dalton et al., 2017)

Deleted: 5
Deleted: 3Kpa
Deleted: 5b
Deleted: two events
Deleted: 5c
Deleted: 5d
Deleted: severe
Deleted: 5e
Deleted: two
Deleted: waves

549

550 Figure 6. Mid-day VPD, Focs, NEE and GPP plotted against the fraction of diffuse
 551 downwelling shortwave radiation (a-d) for early summer, mid-late summer and early fall
 552 of 2015 (these periods are defined in Section 3.4). High values on the x-axis indicate
 553 completely overcast or cloudy conditions, whereas as low values indicated clear skies.
 554 LRU increases with increasing *fdiff* during each period but the increase is most
 555 pronounced in the early summer (e). Gc increases from clear to partly cloudy conditions
 556 across the three periods and plateaus during overcast sky conditions (f). Vertical bars
 557 indicate 1 standard error. Across the three periods, LRU increased with Gc, and levelled
 558 off at Gc values greater than $\sim 0.5 \text{ mol m}^{-2}\text{s}^{-1}$ (g).

559 3.5. Response to heat waves: 2015 was the warmest year in large parts of the Pacific
 560 Northwest since records began in the 1930s (Dalton et al., 2017). We observed three
 561 distinct heat waves during the 2015 summer. These were in early June (DOY 157-160),
 562 end of June- early July (DOY 175-188) and late July-early August (DOY 210-213). The
 563 three heat waves are shown as red, yellow and dark purple lines in Fig. 7; the overall time
 564 series is shown in blue (mid-day means are plotted for all variables). Mid-day
 565 temperatures exceeded 30°C during these heat wave events, while VPD-leaf exceeded 3
 566 kPa during the first heat wave and increased to a maximum of 5.3 kPa during the last
 567 event (Fig. 7b). During the first event, Focs was similar to days immediately prior (Fig.
 568 7c), but the canopy became a net source of CO₂ during all three events (Fig. 7d). The
 569 third events lead to a reduction in Focs, even though the canopy had received some
 570 rainfall in the preceding weeks (Fig. 1c). Water vapor fluxes (Fig. 7e) increased during
 571 the first heat wave, compared to days immediately prior. The increased water vapor flux

is likely ~~form an increase in transpiration under high VPD~~ (red bars in Fig. 7b). Even as canopy conductance (Fig. 7f) is reduced under the ~~third heatwave, high VPD~~, ensures a steady transpirational flux (purple bars in Fig. 7e).

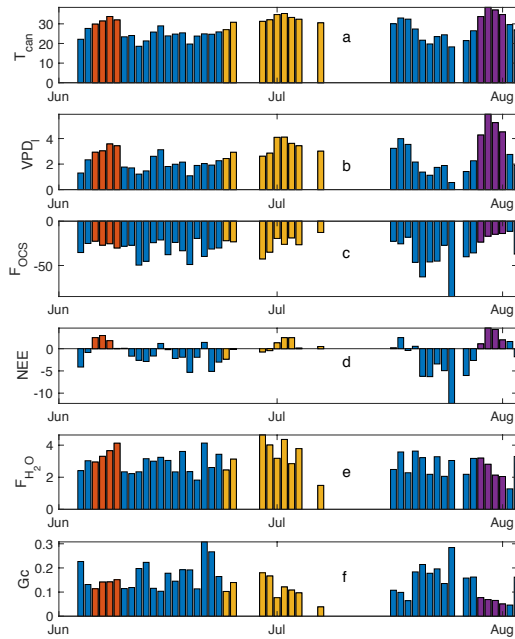
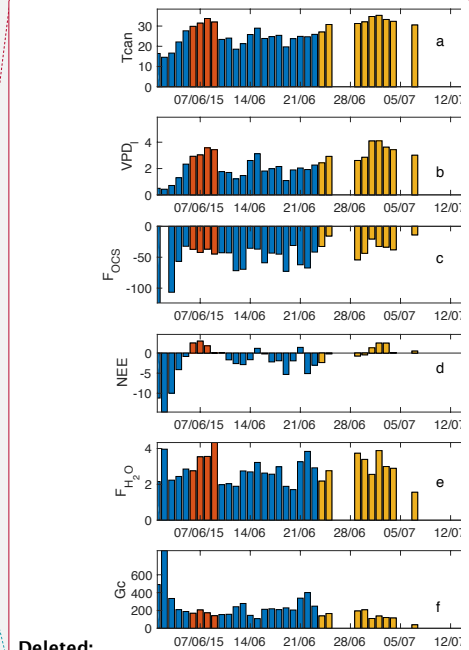


Figure 7. Mid-day means (11am-1pm local time) for three heat wave periods (plotted as red, yellow and purple, while the overall time series is shown in blue). Variables displayed are canopy temperature ($^{\circ}\text{C}$; a), VPD-leaf (b), F_{OCS} (c), NEE (d), water vapor flux (e), and canopy conductance (Gc, f). Units for each panel are the same as specified in previous figures.

4. Conclusions

Over hourly, daily and seasonal timescales, estimates of F_{OCS} generally tracked fluctuations in GPP, implying stomatal control of carbon, water, and OCS fluxes at the site. We used continuous in-situ measurements of OCS mixing ratios, collocated measurements of water vapor fluxes, and air and canopy temperatures to calculate OCS uptake. We found the forest to be a large sink for OCS, with sink strength peaking during daylight hours. The mean LRU was ~ 4 , and varied in response to changing light conditions and canopy conductance. These LRUs are larger than observed from other ecosystem scale studies, but well within the range of reported values (Whelan et al., 2018; Sandoval-Soto et al., 2005). The forest surface was found to be a soil moisture dependent sink of OCS. Ecosystem fluxes of OCS and CO_2 were found to be strongly sensitive to the ratio of diffuse: direct radiation reaching the top of the canopy. Uptake of

~~Deleted: not from increased~~
~~Deleted: ,~~
~~Deleted: scale stomatal~~
~~Deleted: during these events (Gc;~~
~~Deleted: 5f~~
~~Deleted: dramatically~~
~~Deleted: . The increase is rather due to a flux of water from~~
~~Deleted: soil surface and epiphytes that can store water in the canopy. High temperatures during such events are likely to result in increased evaporation.~~



~~Deleted:~~
~~Formatted: Font:(Default) Times New Roman~~
~~Formatted: Font:(Default) Times New Roman~~
~~Deleted: 6~~

~~Deleted: , with magnitudes that were roughly half of nighttime ecosystem fluxes, indicating other components of the ecosystem (epiphytes present throughout the canopy and impartial stomatal closure) to also take up OCS during these hours.~~

626 both OCS and CO₂ increased as sky conditions changed from clear to partly cloudy. A
627 much smaller increase in uptake was observed as sky conditions changed from partly
628 cloudy to overcast, except during the early summer, when soil moisture was not limiting.
629 This change was mediated by the sensitivity of stomata to changing cloudiness and soil
630 moisture, as estimated from canopy conductance. **Finally**, we examined the response of
631 OCS, CO₂ and H₂O fluxes on heatwaves, and found that sequential heatwaves lead to
632 suppression in stomatal gas exchange of all three fluxes.

Deleted: calculated according to the inverted Penman-Monteith equation. Finally

633 Our results support the growing body of work that suggests ecosystem-scale OCS uptake
634 is controlled by stomatal dynamics. While moist old-growth forests in Pacific
635 Northwestern U.S. do not represent a very large fraction of the global terrestrial surface
636 area, results from this study are likely relevant for other old-growth forests, particularly
637 high LAI and very wet forests with extensive epiphyte cover, which are widespread in the
638 humid tropics.

639 Acknowledgements:

640 This work was partly funded by NASA SBIR Phase II award NNX12CD21P to LGR,
641 Inc. (“Ultrasensitive Analyzer for Realtime, In-Situ Airborne and Terrestrial
642 Measurements of OCS, CO₂, and CO.”). We would like to thank the US Forest Service
643 and the University of Washington for letting us use the research facility at Wind River. In
644 particular, we wish to sincerely acknowledge Ken Bible and Matt Schroeder for their help
645 with setting up the experiment as well as maintenance throughout the measurement
646 campaign. Data collected and used in this study can be accessed at
647 ftp.fsl.orst.edu/rastogib/Biogeosciences2018_Rastogi.

648 References:

649 Adams, W. W. and Demmig-Adams, B.: Carotenoid composition and down regulation of
650 photosystem II in three conifer species during the winter, *Physiol. Plant.*, 92(3), 451–458,
651 doi:10.1111/j.1399-3054.1994.tb08835.x, 1994.

652 Alton, P. B., North, P. R. and Los, S. O.: The impact of diffuse sunlight on canopy light-
653 use efficiency, gross photosynthetic product and net ecosystem exchange in three forest
654 biomes, *Glob. Chang. Biol.*, 13(4), 776–787, doi:10.1111/j.1365-2486.2007.01316.x,
655 2007.

656 Asaf, D., Rotenberg, E., Tatarinov, F., Dicken, U., Montzka, S. A. and Yakir, D.:
657 Ecosystem photosynthesis inferred from measurements of carbonyl sulphide flux, *Nat.*
658 *Geosci.*, 6(3), 186–190, doi:10.1038/ngeo1730, 2013.

659 Belviso, S., Reiter, I. M., Loubet, B., Gros, V., Lathièrre, J., Montagne, D., Delmotte, M.,
660 Ramonet, M., Kalogridis, C., Lebegue, B., Bonnaire, N., Kazan, V., Gauquelin, T.,
661 Fernandez, C. and Genty, B.: A top-down approach of surface carbonyl sulfide exchange
662 by a Mediterranean oak forest ecosystem in Southern France, *Atmos. Chem. Phys.*
663 *Discuss.*, (June 2012), 1–25, doi:10.5194/acp-2016-525, 2016.

- 666 Berkelhammer, M., Asaf, D., Still, C., Montzka, S., Noone, D., Gupta, M., Provencal, R.,
667 Chen, H. and Yakir, D.: Constraining surface carbon fluxes using in situ measurements of
668 carbonyl sulfide and carbon dioxide, *Global Biogeochem. Cycles*, 28(2), 161–179,
669 doi:10.1002/2013GB004644, 2014.
- 670 Berkelhammer, M., Steen-Larsen, H. C., Cosgrove, A., Peters, A. J., Johnson, R.,
671 Hayden, M. and Montzka, S. A.: Radiation and atmospheric circulation controls on
672 carbonyl sulfide concentrations in the marine boundary layer, *J. Geophys. Res.*, 121(21),
673 13,113–13,128, doi:10.1002/2016JD025437, 2016.
- 674 Berry, J., Wolf, A., Campbell, J. E., Baker, I., Blake, N., Blake, D., Denning, A. S.,
675 Kawa, S. R., Montzka, S. A., Seibt, U., Stimler, K., Yakir, D. and Zhu, Z.: A coupled
676 model of the global cycles of carbonyl sulfide and CO₂: A possible new window on the
677 carbon cycle, *J. Geophys. Res. Biogeosciences*, 118(2), 842–852,
678 doi:10.1002/jgrg.20068, 2013.
- 679 Billesbach, D. P., Berry, J. A., Seibt, U., Maseyk, K., Torn, M. S., Fischer, M. L., Abu-
680 Naser, M. and Campbell, J. E.: Growing season eddy covariance measurements of
681 carbonyl sulfide and CO₂ fluxes: COS and CO₂ relationships in Southern Great Plains
682 winter wheat, *Agric. For. Meteorol.*, 184, 48–55, doi:10.1016/j.agrformet.2013.06.007,
683 2014.
- 684 [Bloem, E., Haneklaus, S., Kesselmeier, J. and Schnug, E.: Sulfur fertilization and fungal](#)
685 [infections affect the exchange of H₂S and COS from agricultural crops, *J. Agric. Food*](#)
686 [Chem., 60\(31\), 7588–7596, doi:10.1021/jf301912h, 2012.](#)
- 687 Blonquist, J. M., Montzka, S. A., Munger, J. W., Yakir, D., Desai, A. R., Dragoni, D.,
688 Griffis, T. J., Monson, R. K., Scott, R. L. and Bowling, D. R.: The potential of carbonyl
689 sulfide as a proxy for gross primary production at flux tower sites, *J. Geophys. Res.*
690 *Biogeosciences*, 116(4), 1–18, doi:10.1029/2011JG001723, 2011.
- 691 Campbell, J. E., Berry, J., Seibt, U., Smith, S., Nature, S. M.- and 2017, U.: Large
692 historical growth in global terrestrial gross primary production, *nature.com*, 544(7468),
693 84 [online] Available from: <https://www.nature.com/articles/nature22030> (Accessed 29
694 January 2018a), 2017.
- 695 Campbell, J. E., Whelan, M. E., Berry, J. A., Hilton, T. W., Zumkehr, A., Stinecipher, J.,
696 Lu, Y., Kornfeld, A., Seibt, U., Dawson, T. E., Montzka, S. A., Baker, I. T., Kulkarni, S.,
697 Wang, Y., Herndon, S. C., Zahniser, M. S., Commane, R. and Loik, M. E.: Plant Uptake
698 of Atmospheric Carbonyl Sulfide in Coast Redwood Forests, *J. Geophys. Res.*
699 *Biogeosciences*, 122(12), 3391–3404, doi:10.1002/2016JG003703, 2017b.
- 700 Cheng, S. J., Bohrer, G., Steiner, A. L., Hollinger, D. Y., Suyker, A., Phillips, R. P. and
701 Nadelhoffer, K. J.: Variations in the influence of diffuse light on gross primary
702 productivity in temperate ecosystems, *Agric. For. Meteorol.*, 201, 98–110,
703 doi:10.1016/j.agrformet.2014.11.002, 2015.
- 704 Commane, R., Meredith, L. K., Baker, I. T., Berry, J. A., Munger, J. W., Montzka, S. A.,

- 705 Templer, P. H., Juice, S. M., Zahniser, M. S. and Wofsy, S. C.: Seasonal fluxes of
706 carbonyl sulfide in a midlatitude forest, *Proc. Natl. Acad. Sci.*, 112(46), 14162–14167,
707 doi:10.1073/pnas.1504131112, 2015.
- 708 Dalton, M. M., Dello, K. D., Hawkins, L., Mote, P. W. and Rupp, D. E.: The third
709 Oregon climate assessment report, Oregon Clim. Chang. Res. Institute, Coll. Earth,
710 Ocean Atmos. Sci. Oregon State Univ. Corvallis, OR, 2017.
- 711 Eastman, P. A. K. and Camm, E. L.: Regulation of photosynthesis in interior spruce
712 during water stress: changes in gas exchange and chlorophyll fluorescence, *Tree Physiol.*,
713 15(4), 229–235 [online] Available from: <http://dx.doi.org/10.1093/treephys/15.4.229>,
714 1995.
- 715 Falk, M., Wharton, S., Schroeder, M., Ustin, S. L. and Paw U, K. T.: Flux partitioning in
716 an old-growth forest: seasonal and interannual dynamics, *Tree Physiol.*, 28(4), 509–520,
717 doi:10.1093/treephys/28.4.509, 2008.
- 718 Gimeno, T. E., Ogée, J., Royles, J., Gibon, Y., West, J. B., Burlett, R., Jones, S. P.,
719 Sauze, J., Wohl, S., Benard, C., Genty, B. and Wingate, L.: Bryophyte gas-exchange
720 dynamics along varying hydration status reveal a significant carbonyl sulphide (COS)
721 sink in the dark and COS source in the light, *New Phytol.*, 215(3), 965–976,
722 doi:10.1111/nph.14584, 2017.
- 723 Hilton, T., Whelan, M., Zumkehr, A., ... S. K.-N. C. and 2017, U.: Peak growing season
724 gross uptake of carbon in North America is largest in the Midwest USA, *nature.com*,
725 7(6), 450 [online] Available from: <https://www.nature.com/articles/nclimate3272>
726 (Accessed 29 January 2018), 2017.
- 727 Hollinger, A. D. Y., Kelliher, F. M., Byers, J. N., Hunt, J. E., Mcseveny, T. M., Weir, L.,
728 Ecology, S. and Jan, N.: Carbon Dioxide Exchange between an Undisturbed Old-Growth
729 Temperate Forest and the Atmosphere Published by : Wiley Stable URL :
730 <http://www.jstor.org/stable/1939390> REFERENCES Linked references are available on
731 JSTOR for this article : You may need to log , , 75(1), 134–150, 2017.
- 732 Johnson, J. E., Bandy, A. R., Thornton, D. C. and Bates, T. S.: Measurements of
733 atmospheric carbonyl sulfide during the NASA Chemical Instrumentation Test and
734 Evaluation project: Implications for the global COS budget, *J. Geophys. Res.*, 98(D12),
735 23443, doi:10.1029/92JD01911, 1993.
- 736 Kim, Y., Still, C. J., Hanson, C. V., Kwon, H., Greer, B. T. and Law, B. E.: Canopy skin
737 temperature variations in relation to climate, soil temperature, and carbon flux at a
738 ponderosa pine forest in central Oregon, *Agric. For. Meteorol.*, 226–227, 161–173,
739 doi:10.1016/j.agrformet.2016.06.001, 2016.
- 740 Kitz, F., Gerdel, K., Hammerle, A., Laterza, T., Spielmann, F. M. and Wohlfahrt, G.: In
741 situ soil COS exchange of a temperate mountain grassland under simulated drought,
742 *Oecologia*, 183(3), 851–860, doi:10.1007/s00442-016-3805-0, 2017.

Deleted: Dawson, T., Burgess, S., Tu, K., ... R. O.-T. and 2007, U.: Nighttime transpiration in woody plants from contrasting ecosystems., *Tree Physiol.*, 27, 561–575, 2007. .

Deleted: Harmon, M., Bible, K., Ryan, M., Shaw, D., Chen, H., Klopatek, J. and Li, X.: Production, Respiration, and Overall Carbon Balance in an Old-growth Pseudotsuga-Tsuga Forest Ecosystem, *Ecosystems*, 498–512, doi:10.1007/s10021-004-0140-9, 2004. .

- 751 Kooijmans, L. M. J. J., Maseyk, K., Seibt, U., Sun, W., Vesala, T., Mammarella, I.,
752 Kolari, P., Aalto, J., Franchin, A., Vecchi, R., Valli, G. and Chen, H.: Canopy uptake
753 dominates nighttime carbonyl sulfide fluxes in a boreal forest, *Atmos. Chem. Phys.*,
754 17(18), 11453–11465, doi:10.5194/acp-17-11453-2017, 2017.
- 755 Launois, T., Peylin, P., Belviso, S. and Poulter, B.: A new model of the global
756 biogeochemical cycle of carbonyl sulfide - Part 2: Use of carbonyl sulfide to constrain
757 gross primary productivity in current vegetation models, *Atmos. Chem. Phys.*, 15(16),
758 9285–9312, doi:10.5194/acp-15-9285-2015, 2015.
- 759 Maseyk, K., Berry, J. A., Billesbach, D., Campbell, J. E., Torn, M. S., Zahniser, M. and
760 Seibt, U.: Sources and sinks of carbonyl sulfide in an agricultural field in the Southern
761 Great Plains, *Proc. Natl. Acad. Sci.*, 111(25), 9064–9069, doi:10.1073/pnas.1319132111,
762 2014.
- 763 Notholt, J., Kuang, Z., Rinsland, C. P., Toon, G. C., Rex, M., Jones, N., Albrecht, T.,
764 Deckelmann, H., Krieg, J. and Weinzierl, C.: Enhanced upper tropical tropospheric COS:
765 Impact on the stratospheric aerosol layer, *Science* (80-.), 300(5617), 307–310, 2003.
- 766 Parker, G. G., Harmon, M. E., Lefsky, M. A., Chen, J., Pelt, R. Van, Weis, S. B.,
767 Thomas, S. C., Winner, W. E., Shaw, D. C. and Frankling, J. F.: Three-dimensional
768 Structure of an Old-growth Pseudotsuga-Tsuga Canopy and Its Implications for Radiation
769 Balance, Microclimate, and Gas Exchange, *Ecosystems*, 7(5), 440–453,
770 doi:10.1007/s10021-004-0136-5, 2004.
- 771 Paw U, K. T., Falk, M., Suchanek, T. H., Ustin, S. L., Chen, J., Park, Y.-S., Winner, W.
772 E., Thomas, S. C., Hsiao, T. C., Shaw, R. H., King, T. S., Pyles, R. D., Schroeder, M. and
773 Matista, A. A.: Carbon Dioxide Exchange between an Old-Growth Forest and the
774 Atmosphere, *Ecosystems*, 7(5), 513–524, doi:10.1007/s10021-004-0141-8, 2004.
- 775 Protoschill-Krebs, G Wilhelm, C Kesselmeier, J.: Consumption of carbonyl sulphide
776 (COS) by higher plant carbonic anhydrase (CA), *Atmos. Environ.*, 30(18), 3151–3156
777 [online] Available from:
778 <https://www.sciencedirect.com/science/article/pii/S135223109600026X> (Accessed 29
779 January 2018), 1996.
- 780 Protoschill - Krebs, G. and Kesselmeier, J.: Enzymatic pathways for the consumption of
781 carbonyl sulphide (COS) by higher plants, *Bot. Acta*, 105, 206–212 [online] Available
782 from: <http://onlinelibrary.wiley.com/doi/10.1111/j.1438-8677.1992.tb00288.x/full>
783 (Accessed 29 January 2018), 1992.
- 784 [Reichstein, M., Falge, E., Baldocchi, D., Papale, D., Aubinet, M., Berbigier, P.,](#)
785 [Bernhofer, C., Buchmann, N., Gilmanov, T. and Granier, A.: On the separation of net](#)
786 [ecosystem exchange into assimilation and ecosystem respiration: review and improved](#)
787 [algorithm, *Glob. Chang. Biol.*, 11\(9\), 1424–1439, 2005.](#)
- 788 Sandoval-Soto, L., Stanimirov, M., von Hobe, M., Schmitt, V., Valdes, J., Wild, A. and
789 Kesselmeier, J.: Global uptake of carbonyl sulfide (COS) by terrestrial vegetation:

Deleted: Monteith, J. L.: Evaporation and environment, in
Symp. Soc. Exp. Biol, vol. 19, p. 4., 1965. .

Formatted: Font:Calibri

- 792 Estimates corrected by deposition velocities normalized to the uptake of carbon dioxide,
793 (CO₂), *Biogeosciences Discuss.*, 2(1), 183–201, doi:10.5194/bgd-2-183-2005, 2005.
- 794 Seibt, U., Kesselmeier, J., Sandoval-Soto, L., Kuhn, U. and Berry, J. A.: A kinetic
795 analysis of leaf uptake of COS and its relation to transpiration, photosynthesis and carbon
796 isotope fractionation, *Biogeosciences*, 7(1), 333–341, doi:10.5194/bg-7-333-2010, 2010.
- 797 Shaw, D., Franklin, J., Bible, K., Klopatek, J., Freeman, E., Greene, S. and Parker, G.:
798 Ecological Setting of the Wind River Old-growth Forest, *Ecosystems*, 7(5), 427–439,
799 doi:10.1007/s10021-004-0135-6, 2004.
- 800 Stimler, K., Nelson, D. and Yakir, D.: High precision measurements of atmospheric
801 concentrations and plant exchange rates of carbonyl sulfide using mid-IR quantum
802 cascade laser, *Glob. Chang. Biol.*, 16(9), 2496–2503, doi:10.1111/j.1365-
803 2486.2009.02088.x, 2010a.
- 804 Stimler, K., Montzka, S. A., Berry, J. A., Rudich, Y. and Yakir, D.: Relationships
805 between carbonyl sulfide (COS) and CO₂ during leaf gas exchange, *New Phytol.*, 186(4),
806 869–878, doi:10.1111/j.1469-8137.2010.03218.x, 2010b.
- 807 Sun, W., Maseyk, K., Lett, C. and Seibt, U.: Litter dominates surface fluxes of carbonyl
808 sulfide in a Californian oak woodland, *J. Geophys. Res. G Biogeosciences*, 121(2), 438–
809 450, doi:10.1002/2015JG003149, 2016.
- 810 Urban, O., Janouš, D., Acosta, M., Czerný, R., Marková, I., Navrátil, M., Pavelka, M.,
811 Pokorný, R., Šprtová, M., Zhang, R., Špunda, V. R., Grace, J. and Marek, M. V.:
812 Ecophysiological controls over the net ecosystem exchange of mountain spruce stand.
813 Comparison of the response in direct vs. diffuse solar radiation, *Glob. Chang. Biol.*,
814 13(1), 157–168, doi:10.1111/j.1365-2486.2006.01265.x, 2007.
- 815 Wehr, R., Commane, R., Munger, J. W., Barry Mcmanus, J., Nelson, D. D., Zahniser, M.
816 S., Saleska, S. R. and Wofsy, S. C.: Dynamics of canopy stomatal conductance,
817 transpiration, and evaporation in a temperate deciduous forest, validated by carbonyl
818 sulfide uptake, *Biogeosciences*, 14(2), 389–401, doi:10.5194/bg-14-389-2017, 2017.
- 819 Wharton, S. and Falk, M.: Climate indices strongly influence old-growth forest carbon
820 exchange, *Environ. Res. Lett.*, 11(4), 1–11, doi:10.1088/1748-9326/11/4/044016, 2016.
- 821 Wharton, S., Falk, M., Bible, K., Schroeder, M. and Paw U, K. T.: Old-growth CO₂ flux
822 measurements reveal high sensitivity to climate anomalies across seasonal, annual and
823 decadal time scales, *Agric. For. Meteorol.*, 161, 1–14,
824 doi:10.1016/j.agrformet.2012.03.007, 2012.
- 825 Whelan, M. E., Hilton, T. W., Berry, J. A., Berkelhammer, M., Desai, A. R. and
826 Campbell, J. E.: Carbonyl sulfide exchange in soils for better estimates of ecosystem
827 carbon uptake, *Atmos. Chem. Phys.*, 16(6), 3711–3726, 2016.
- 828 Whelan, M. E., Lennartz, S. T., Gimeno, T. E., Wehr, R., Wohlfahrt, G., Wang, Y.,

Deleted: ,

Deleted: Discuss., 6

Deleted: bgd-6-9279-2009

- 832 Kooijmans, L. M. J., Hilton, T. W., Belviso, S., Peylin, P., Commane, R., Sun, W., Chen,
833 H., Kuai, L., Mammarella, I., Maseyk, K., Berkelhammer, M., Li, K.-F., Yakir, D.,
834 Zumkehr, A., Katayama, Y., Ogée, J., Spielmann, F. M., Kitz, F., Rastogi, B.,
835 Kesselmeier, J., Marshall, J., Erkkilä, K.-M., Wingate, L., Meredith, L. K., He, W., Bunk,
836 R., Launois, T., Vesala, T., Schmidt, J. A., Fichot, C. G., Seibt, U., Saleska, S., Saltzman,
837 E. S., Montzka, S. A., Berry, J. A. and Campbell, J. E.: Reviews and Syntheses: Carbonyl
838 Sulfide as a Multi-scale Tracer for Carbon and Water Cycles, *Biogeosciences Discuss.*,
839 (October), 1–97, doi:10.5194/bg-2017-427, 2017.
- 840 Winner, W., Thomas, S., Berry, J., Bond, B., Cooper, C., Hinckley, T., Ehleringer, J.,
841 Fessenden, J., Lamb, B., McCarthy, S., McDowell, N., Phillips, N. and Williams, M.:
842 Canopy Carbon Gain and Water Use: Analysis of Old-growth Conifers in the Pacific
843 Northwest, *Ecosystems*, 7(5), 482–497, doi:10.1007/s10021-004-0139-2, 2004.
- 844 Wohlfahrt, G., Brilli, F., Hörtnagl, L., Xu, X., Bingemer, H., Hansel, A. and Loreto, F.:
845 Carbonyl sulfide (COS) as a tracer for canopy photosynthesis, transpiration and stomatal
846 conductance: Potential and limitations, *Plant, Cell Environ.*, 35(4), 657–667,
847 doi:10.1111/j.1365-3040.2011.02451.x, 2012.
- 848 Woodruff, D. R., McCulloh, K. A., Warren, J. M., Meinzer, F. C. and Lachenbruch, B.:
849 Impacts of tree height on leaf hydraulic architecture and stomatal control in Douglas-fir,
850 *Plant, Cell Environ.*, 30(5), 559–569, doi:10.1111/j.1365-3040.2007.01652.x, 2007.
- 851

where e_s is saturation vapor pressure at the leaf surface (kPa), using leaf skin temperature, e_a is the actual vapor pressure (kPa), P is the measured atmospheric pressure (Pa) at the tower top, and $\chi_{H_2O}^l$ and $\chi_{H_2O}^a$ (ppth) are the leaf and ambient H_2O mixing ratios at the canopy top. Finally, since gradients of OCS and H_2O are estimated between ambient air and the leaf intercellular spaces, these are normalized by the ratio of diffusivities of these two species in air (Seibt et al., 2010; Wohlfahrt et al., 2012).

F_{H_2O} was measured using eddy covariance at the tower top (70m). In high LAI forests with minimal exposed soil, such as those of the Pacific Northwest, fluxes of F_{H_2O} can be treated as a good proxy for transpiration, since soil evaporation should be minimal. We excluded rainy days, as well as two days following rainfall, to only capture periods when F_{H_2O} can be assumed to be dominated by transpiration. We included nighttime data since several temperate tree species are known to transpire during the night (Dawson et al., 2007). Moreover, in this particular forest OCS is taken up by epiphytes under conditions of high humidity, which are common at nighttime (Rastogi et al., in revision). The first term in right hand side of equation (1) was evaluated only under the condition $F_{H_2O} > 0.2 \text{ mmolm}^{-2}\text{s}^{-1}$. When this condition was not met (e.g. at nighttime), fluxes were calculated using by integrating the rate of change in hourly OCS mixing ratios through the entire profile.

where GPP was estimated from CO_2 fluxes measured at the tower top. Finally, canopy conductance (G_c) was calculated by inverting the Penman Monteith equation (Monteith, 1965), which uses a combination of micrometeorological and eddy flux data collected above the canopy at the tower top. G_c is the canopy-scale equivalent of stomatal conductance, with the assumption that the canopy (or ecosystem) acts as a single big leaf.

$$G_c = \left[\frac{\rho C_p \delta e}{\gamma L e} + \frac{\left(\frac{\Delta}{\gamma}\right)^{\beta-1}}{G_a} \right]^{-1}, \quad (6)$$

where ρ is air density (kg m^{-3}), C_p is specific heat ($\text{J kg}^{-1}\text{K}^{-1}$), δe is vapor pressure deficit (kPa), γ is the psychrometric constant (kPa K^{-1}), Δ is the slope of the saturation vapor pressure curve (kPa K^{-1}), β is the Bowen ratio (H:LE), and G_a is the aerodynamic conductance for momentum transfer, calculated as $u^* \cdot u^{-1}$

(where u^* is the friction velocity calculated from the momentum fluxes and u is the horizontal wind speed). G_a provides a measure of how well the canopy top is coupled to the background atmosphere (Wharton et al., 2012).

At the peak of the soil drought (August; Fig. 1d), nighttime ecosystem OCS flux was similar to the chamber-based surface fluxes, after which magnitudes differed by a factor of 2-3. This difference can be explained by epiphytic consumption of OCS. Epiphytes are a moisture dependent sink OCS at the site (Rastogi et al., in revision) and therefore are likely inactive during the warmest and driest part of the year. Surface fluxes of CO_2 on the other hand were much higher than ER estimated from the flux tower (blue circles in Fig. 4b). While there are issues in scaling up chamber-based estimates, these results corroborate earlier work that suggest that flux tower based estimates of ER at this site might be underestimated (Harmon et al., 2004).

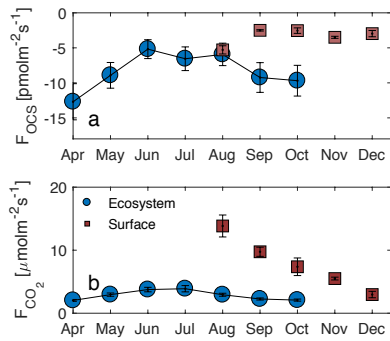


Figure 4. Nighttime ecosystem F_{OCS} and F_{CO_2} (blue circles in a-b) and

The diffuse light enhancement of stomatal and canopy conductance is well documented across a range of forest ecosystems (Alton et al., 2007; Cheng et al., 2015; Hollinger et al., 2017; Urban et al., 2007; Wharton et al., 2012). Lower VPD (Fig. 5a) and light levels allow plants to keep stomata open at mid-day and continue fixing CO_2 . Lower VPD reduces transpirational losses, and the lack of VPD-induced partial stomatal closure reduces the resistance to CO_2 diffusion into the leaf. Correspondingly, the less directional nature of diffuse solar radiation allows greater penetration into the canopy, thus increasing photosynthesis across the entire canopy, even as a reduction in canopy top leaf photosynthesis is observed due to a reduction in total radiation. In a multi-year analysis at Wind River, Wharton et al., (2012) found that cloudy and partly cloudy sky conditions during the peak-growing season lead to an enhancement of NEE. During our study, G_c was generally higher in the early growing season, but increased as sky conditions changed from clear skies to overcast. This increase was similar across the three time periods, even as the response of OCS and CO_2 fluxes was different across these periods. This indicates that declining soil moisture (Fig. 1d) likely limits gas exchange as the summer progresses, even as canopy conductance can be reasonably high under overcast skies.

